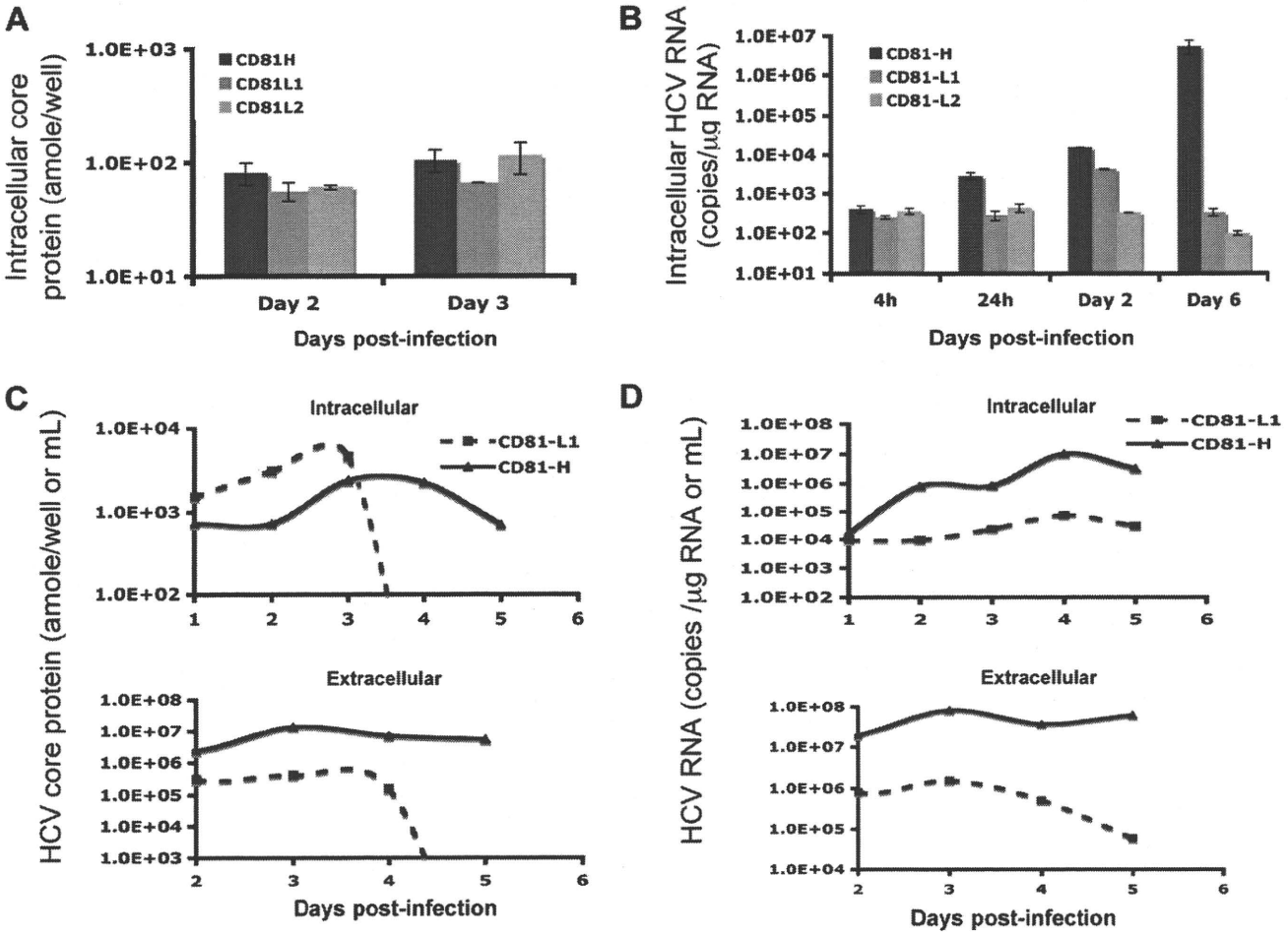

FIG. 5. HCV core protein and HCV RNA levels in the three CD81 cell populations. (A) Intracellular core protein levels of infected CD81-H, CD81-L1, and CD81-L2 cells were determined by ELISA at days 2 and 3 p.i. (B) Intracellular HCV RNA levels of the three cell lines were measured by q-RT-PCR. (C and D) Intracellular (top) and extracellular (bottom) core (C) and HCV RNA (D) levels at various time points p.i. were measured. Mean values ± SD are shown. Data from one of three independent experiments are shown.

HCV to replicate efficiently in CD81-L2 is a result of low levels of CD81 expression. This experiment also supports the above-described finding that HCV can enter into CD81-low cells but fails to initiate replication efficiently.

Huh7-25 cells were also tested in this replicon transfection experiment. As shown in Fig. 6C, JFH1 subgenomic replicon RNA replicated efficiently only in Huh7-25 cells transfected with CD81 DNA but not in cells with vector DNA or no DNA transfection, confirming that the Huh7-25 clone behaves like CD81-L2 cells in these experiments. Like CD81-L2 cells, Huh7-25 cells showed little virus production after infection with JFH-1 HCVcc. However, robust viral production was detected in infected Huh7-25 cells that were later transfected with the CD81 expression plasmid (Fig. 6D). To determine that CD81-mediated entry did not account for this increase, CD81-blocking antibody was added to the medium after transfection. CD81-H cells were used as a control and showed that the addition of CD81 antibodies after infection substantially inhibited viral spread (Fig. 6D, top), suggesting that the recently reported CD81-independent cell-to-cell transmission (45, 47) does not play a major role here. In contrast, Huh7-25 cells transfected with CD81 showed a substantial increase (2 logs) in HCV RNA levels despite the addition of CD81 antibodies on the day of CD81 transfection (Fig. 6D, bottom). A further increase (1 log) without the addition of CD81 antibodies after CD81 transfection was noted, probably due to the effect on viral spread.

Modulation of HCV replication by CD81 in HCV replicon cells. To further study the effect of CD81 expression on HCV replication, several subgenomic replicon cells (25, 43) were studied. Since subgenomic replicon cells harbor HCV RNA sequences covering only the NS3-NS5 region, infectious virus is not produced and viral spread does not occur. The HCV RNA level in a JFH1 subgenomic replicon cell line with low CD81 levels (pSGR-JFH1-C4/1) (25) (see Fig. S4B in the supplemental material) was studied by transiently transfecting a CD81 expression plasmid. After CD81 transfection, a 3- to 6-fold increase in HCV RNA levels was observed for this cell line (Fig. 7A). Control transfection with an empty vector or a CD81 mutant had no effect on HCV replication.

Two other subgenomic replicon cell lines, Huh7/Rep-Feo (genotype 1b) (43) and SGR-JFH1-FLuc/Neo (genotype 2a),

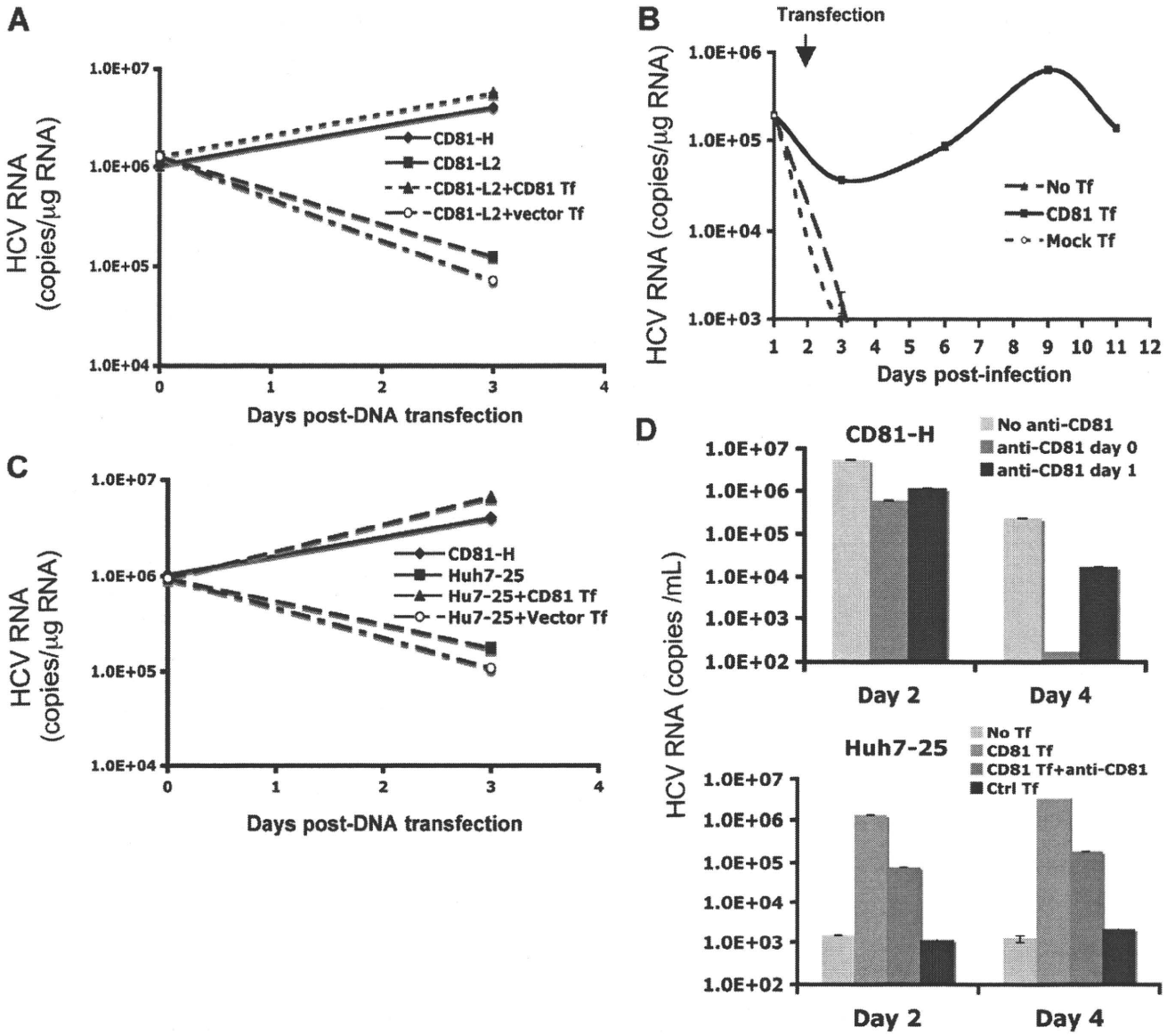

FIG. 6. Transient expression of CD81 restores HCV RNA replication in CD81-L2 and Huh7-25 cells. (A) JFH1 subgenomic HCV RNA (pSGR-JFH1/Luc) was transfected into CD81-H or -L2 cells in triplicate followed by the transfection of a CD81 expression plasmid (CD81-L2+CD81 Tf) or a control plasmid (CD81-L2+Vector Tf) 24 h later. HCV RNA was harvested, and levels were determined immediately and 2 days after CD81 transfection. (B) CD81-L2 cells were infected with HCVcc and 24 h later were transfected with a CD81 expression plasmid. The amount of intracellular HCV RNA was then quantified at various time points. No Tf, no transfection; Control Tf, transfection with a control plasmid. (C) JFH1 subgenomic HCV RNA was transfected into Huh7-25 cells in triplicate, followed by the transfection of a CD81 expression plasmid (Huh7-25+CD81 Tf) or a control plasmid (Huh7-25+Vector Tf) 24 h later. HCV RNA was harvested, and levels were determined immediately and 2 days after CD81 transfection. (D) CD81-H (top) and Huh7-25 (bottom) cells were infected with HCVcc, and Huh7-25 cells were transfected with a CD81 expression plasmid 24 h later. Both cells were treated with anti-CD81 antibody at various time points (anti-CD81 day 0, anti-CD81 antibody was added together with HCVcc; anti-CD81 day 1, CD81 antibody was added on day 1 p.i; CD81 Tf, HCVcc infection followed by transfection with CD81 1 day later; CD81 Tf+anti-CD81, HCVcc infection followed by transfection of CD81 1 day later with the addition of anti-CD81). HCV RNA levels in the culture supernatant were determined at various time points. Data from one of three independent experiments are shown.

had high levels of CD81 expression (see Fig. S4C and S4D in the supplemental material) and were treated with CD81 siRNA (Dharmacon) to reduce CD81 expression levels by 80% or more. The HCV RNA level was reduced by 4- to 6-fold in CD81 siRNA-transfected cells, whereas control siRNA transfection had no effect (Fig. 7B and C). The data showed that the replications of both JFH1 genotype 2a and 1b RNAs are CD81 dependent. The lowering of the HCV RNA level as a result of the specific reduction in the level of CD81 by siRNA confirmed the causative relationship between the CD81 level and the HCV replication efficiency.

CD81-dependent HCV RNA replication was further illustrated by the kinetics of HCV RNA and CD81 RNA levels in genotype 1b and 2a subgenomic replicon cells with high levels

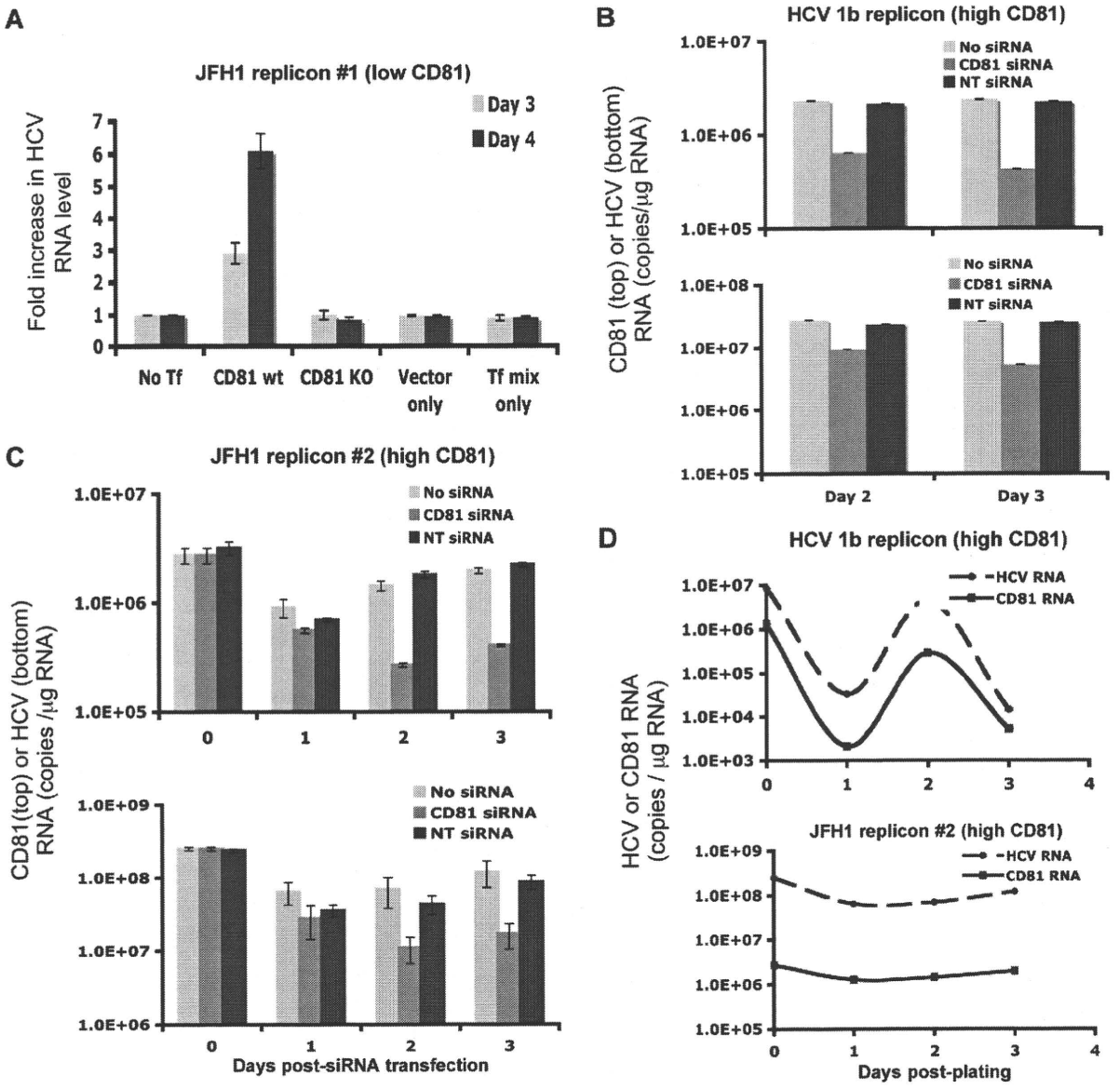

FIG. 7. Modulation of the CD81 level changes HCV RNA replication efficiency. (A) JFH1 subgenomic replicon cells with low CD81 levels (pSGR-JFH1-C4/1) were transfected with a CD81 expression plasmid, and HCV RNA levels were determined on days 3 and 4 after transfection. The fold increase in the HCV RNA level after transfection is shown. CD81 KO, CD81 plasmid with a mutated start codon. (B and C) Two HCV subgenomic replicon cell lines, Huh7/Rep-Feo (B) and SGR-JFH1-FLuc/Neo (C), both of which have high levels of CD81 expression, were treated with CD81 siRNA to silence CD81 expression. CD81 RNA (top) and HCV RNA (bottom) levels were determined 2 and 3 days later. NC, negative control (nontargeted 2) siRNA. (D) CD81 and HCV RNA levels were determined in 1b (top) and JFH 2 (bottom) subgenomic replicon cells at various time points after plating. Mean values ± SD are shown. Data from one of three independent experiments are shown.

of CD81 expression. CD81 levels in those cells fluctuated, and so did the HCV RNA levels. A positive correlation between the two kinetics was observed (Fig. 7D), suggesting the importance of high levels of CD81 for efficient HCV replication.

CD81 in HCV RNA template function. Like other positive-strand RNA viruses, the use of the same viral RNA as templates by viral protein translation and RNA transcription in the HCV life cycle should be mutually exclusive. The experimental data supporting this notion for positive-strand RNA viruses were generated from an *in vitro* cell-free system (4, 15). The template pool is constantly replenished as *in vivo* infection proceeds, and the two processes are expected to be asynchronous. However, a clear pattern for a single dominant template function at a time would also be predicted if the template function is subjected to control by a cellular factor(s) allowing coordinated protein translation and RNA transcription. Indeed, we observed a pattern for the mutually exclusive use of HCV RNA as templates for viral protein translation versus RNA replication in infected cell cultures when the kinetics of HCV RNA and core protein levels were analyzed. As shown in Fig. 8, the kinetics of the intracellular HCV RNA and core protein levels were opposite at each time point: an increasing

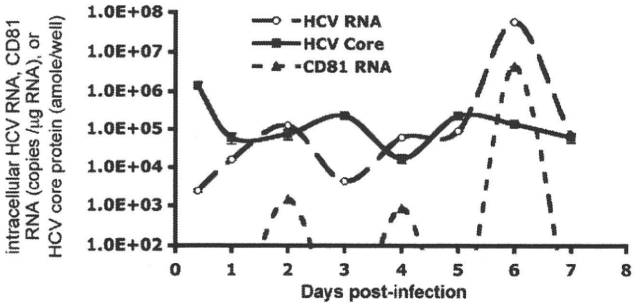

FIG. 8. Relationship of intracellular HCV RNA and core protein levels to CD81 levels during viral replication. CD81-H cells were infected with HCV and harvested at various time points. Intracellular HCV RNA, CD81 RNA, and core protein levels were determined. amole/well, attomoles/well. Mean values ± SD are shown. Data from one of two independent experiments are shown.

intracellular HCV RNA level was accompanied by a decreasing core protein level and vice versa. Our data not only support the mutually exclusive use of HCV RNA for each template function *in vivo* but also suggest that cellular factors may direct HCV RNA to one template function at a time. When the kinetics of the intracellular HCV RNA, core protein, and CD81 levels were analyzed, changing CD81 RNA levels were positively correlated with the changing HCV RNA level but were inversely related to the core protein level (Fig. 8). The positive and inverse correlations among CD81, HCV RNA, and viral protein kinetics suggest that CD81 may be one of the cellular factors directing HCV RNA to the replication process. The viral protein level appears normal while the HCV RNA level is decreasing when the CD81 level is low, suggesting that templates can still be used for viral protein translation but not for RNA synthesis. This is probably why no difference in the luciferase activities or core protein levels in CD81-L cells from those in CD81-H was detected at the early phase of transfection or infection. Thus, CD81 may control HCV RNA replication, possibly through directing HCV RNA template function toward RNA replication.

DISCUSSION

CD81 is known to mediate viral entry in HCV infection (10, 30, 34, 49) and was also implicated in the cell-to-cell transmission of HCV infection (45, 47). Our study showed that significant differences existed in HCV RNA levels after HCV infection among CD81-H, CD81-L1, and CD81-L2 populations and could not be explained simply by the CD81 entry function. This observation prompted us to investigate whether CD81 is required for additional steps in the HCV life cycle, such as RNA replication. Using a variety of techniques and cell lines, we uncovered a novel function of CD81 in the HCV life cycle that is important for HCV RNA replication. CD81 is a tetraspanin family member and is enriched in the lipid rafts of membranous compartments of the cell, where HCV RNA replication is believed to take place (9, 16). The requirement for CD81 participation by the HCV replication process can be facilitated by the physical proximity of CD81 to the HCV replicating site.

To explain our data and the proposed dual functions of CD81 in the context of HCV infection and replication, we reason that a low threshold amount of CD81 is required for the HCV entry function but that a much higher level of CD81 is necessary for efficient HCV replication subsequent to viral entry. Koutsoudakis et al. (26) previously reported that about 70,000 CD81 molecules in a cell appear to be the threshold for viral entry. Our data suggest that the three cell lines with very different levels of CD81 allow similar viral entry but appear to support divergent efficiencies of HCV replication that correlate well with CD81 levels. It is interesting that CD81-L2 cells, despite having very low levels of CD81, can still support viral entry although at a somewhat lower level than the higher-level-CD81-expressing cells. The CD81 expression level of the L2 cells is probably just around the "threshold level" for viral entry.

Our data provide evidence for the mutually exclusive use of HCV RNA as templates for either RNA replication or protein synthesis in infected cell cultures. Two lines of evidence support that the use of HCV RNA for RNA replication is subjected to cellular factor control, such as CD81. One line of evidence is the absence of efficient RNA replication after viral protein translation in HCV-infected and RNA-transfected CD81-L1 and -L2 cells, suggesting that RNA replication could not occur efficiently when the CD81 level was low. The other evidence is that a clear pattern for one dominant template function at a time was shown for infected CD81-H cells, suggesting that there is a coordinated process that directs HCV RNA molecules toward RNA replication function. It is likely that cellular factors are involved in directing viral RNA molecules toward two distinct template functions. On the other hand, viral protein synthesis is negatively correlated with CD81 and HCV RNA levels. These data suggest that the template function of HCV RNA is controlled by cellular factors like CD81, which directs HCV RNA toward its replication function instead of protein translation. However, it is not clear how CD81 exerts this function.

CD81 may assist directly in the assembly of the HCV replicase complex, including NS5B, contributing to viral RNA replication. Alternatively, CD81 may be linked indirectly to a cellular pathway that is critical for efficient viral replication. In a recent study, Brazzoli et al. showed that the engagement of CD81 during HCV infection activates the Raf/MEK/extracellular signal-regulated kinase (ERK) signaling cascade and that this pathway affects postentry events of the HCV life cycle, presumably at the replication step (8). Further experiments are needed to elucidate the molecular mechanism of this novel CD81 function.

CD81 was previously reported to have diverse functions in biological process. For instance, CD81 is implicated in the metastasis of cancer cells (21). CD81 can influence the adhesion, morphology, activation, proliferation, and differentiation of B, T, and other cells (22). In parasite infections, hepatocyte CD81 is required for *Plasmodium falciparum* and *Plasmodium yoelii* sporozoite infectivity (39). CD81 was also implicated in the modulation of infectivity, enhancement of viral gene expression, and promotion of virus assembly, budding, and cell-to-cell spread in the HIV life cycle (19, 38, 44). The identification of this novel CD81 function in HCV replication indicates that CD81 plays a more pleiotropic role in the HCV life cycle besides its well-defined role in viral entry. Our data

suggest that CD81 has dual functions in HCV infection: a low threshold level of CD81 required for viral entry and a higher level of CD81 necessary for efficient HCV RNA replication. The dependence of HCV replication on CD81 creates an inherent vulnerability for HCV replication. Thus, CD81 functions could be explored for potential therapeutic development because of the multiple roles of CD81 in HCV infection, as was explored in a recent study of the Alb-uPA/SCID mouse model engrafted with human hepatocytes (29).

ACKNOWLEDGMENTS

We thank Matthew Evans and Charlie Rice for providing the J6/JFH1p7Rluc2A plasmid and H77 HCVpp and Huh 7.5 cells, Shoshana Levy for the human CD81 plasmid, Michael Niepmann for the pHCV-FLuc-3′-UTR plasmid, Takanobu Kato and Takaji Wakita for the Huh7-25 and SGR-JFH1-C4/1 cell lines, and Naoya Sakamoto for the Huh7/Rep-Feo cell line.

This study was supported by the Intramural Research Program of NIDDK, National Institutes of Health.

REFERENCES

1. **Akazawa, D., T. Date, K. Morikawa, A. Murayama, M. Miyamoto, M. Kaga, H. Barth, T. F. Baumert, J. Dubuisson, and T. Wakita.** 2007. CD81 expression is important for the permissiveness of Huh7 cell clones for heterogeneous hepatitis C virus infection. J. Virol. **81:**5036–5045.
2. **Alter, M. J.** 2007. Epidemiology of hepatitis C virus infection. World J. Gastroenterol. **13:**2436–2441.
3. **Bartenschlager, R., M. Frese, and T. Pietschmann.** 2004. Novel insights into hepatitis C virus replication and persistence. Adv. Virus Res. **63:**71–180.
4. **Barton, D. J., B. J. Morasco, and J. B. Flanegan.** 1999. Translating ribosomes inhibit poliovirus negative-strand RNA synthesis. J. Virol. **73:**10104–10112.
5. **Bartosch, B., C. Logvinoff, C. M. Rice, and J. A. McKeating.** 2003. Cell entry of hepatitis C virus requires a set of co-receptors that include the CD81 tetraspanin and the SR-B1 scavenger receptor. J. Biol. Chem. **278:**41624–41630.
6. **Bartosch, B., J. Dubuisson, and F. L. Cosset.** 2003. Infectious hepatitis C virus pseudo-particles containing functional E1-E2 envelope protein complexes. J. Exp. Med. **197:**633–642.
7. **Blight, K. J., J. A. McKeating, and C. M. Rice.** 2002. Highly permissive cell lines for subgenomic and genomic hepatitis C virus RNA replication. J. Virol. **76:**13001–13014.
8. **Brazzoli, M. A. Bianchi, S. Filippini, A. Weiner, Q. Zhu, M. Pizza, and S. Crotta.** 2008. CD81 is a central regulator of cellular events required for hepatitis C virus infection of human hepatocytes. J. Virol. **82:**8316–8329.
9. **Claas, C., C. S. Stipp, and M. E. Hemler.** 2001. Evaluation of prototype transmembrane 4 superfamily protein complexes and their relation to lipid rafts. J. Biol. Chem. **276:**7974–7984.
10. **Cormier, E. G., F. Tsamis, F. Kajumo, R. J. Durso, J. P. Gardner, and T. Dragic.** 2004. CD81 is an entry coreceptor for hepatitis C virus. Proc. Natl. Acad. Sci. U. S. A. **101:**7270–7274.
11. **Evans, M. J., T. von Hahn, D. M. Tscherne, A. J. Syder, M. Panis, B. Wölk, T. Hatziioannou, J. A. McKeating, P. D. Bieniasz, and C. M. Rice.** 2007. Claudin-1 is a hepatitis C virus co-receptor required for a late step in entry. Nature **446:**801–805.
12. **Feld, J. J., and J. H. Hoofnagle.** 2005. Mechanism of action of interferon and ribavirin in treatment of hepatitis C. Nature **436:**967–972.
13. **Feld, J. J., and T. J. Liang.** 2005. HCV persistence: cure is still a four letter word. Hepatology **41:**23–25.
14. **Flint, M., C. Logvinoff, C. M. Rice, and J. A. McKeating.** 2004. Characterization of infectious retroviral pseudotype particles bearing hepatitis C virus glycoproteins. J. Virol. **78:**6875–6882.
15. **Gamarnik, A. V., and R. Andino.** 1998. Switch from translation to RNA replication in a positive-stranded RNA virus. Genes Dev. **12:**2293–2304.
16. **Gao, L., H. Aizaki, J. W. He, and M. M. Lai.** 2004. Interactions between viral nonstructural proteins and host protein hVAP-33 mediate the formation of hepatitis C virus RNA replication complex on lipid raft. J. Virol. **78:**3480–3488.
17. **Haberstroh, A., E. K. Schnober, M. B. Zeisel, P. Carolla, H. Barth, H. E. Blum, F. L. Cosset, G. Koutsoudakis, R. Bartenschlager, A. Union, E. Depla, A. Owsianka, A. H. Patel, C. Schuster, F. Stoll-Keller, M. Doffoël, M. Dreux, and T. F. Baumert.** 2008. Neutralizing host responses in hepatitis C virus infection target viral entry at postbinding steps and membrane fusion. Gastroenterology **135:**1719–1728.
18. **Hoofnagle, J. H.** 2002. Course and outcome of hepatitis C. Hepatology **36:**S21–S29.
19. **Jolly, C., and Q. J. Sattentau.** 2007. Human immunodeficiency virus type 1 assembly, budding, and cell-cell spread in T cells take place in tetraspanin-enriched plasma membrane domains. J. Virol. **81:**7873–7884.
20. **Jones, C. T., C. L. Murray, D. K. Eastman, J. Tassello, and C. M. Rice.** 2007. Hepatitis C virus p7 and NS2 proteins are essential for production of infectious virus. J. Virol. **81:**8374–8383.
21. **Le Naour, F., M. André, C. Greco, M. Billard, B. Sordat, J. F. Emile, F. Lanza, C. Boucheix, and E. Rubinstein.** 2006. Profiling of the tetraspanin web of human colon cancer cells Mol. Cell. Proteomics **5:**845–857.
22. **Levy, S., S. C. Todd, and H. T. Maecker.** 1998. CD81 (TAPA-1): a molecule involved in signal transduction and cell adhesion in the immune system. Annu. Rev. Immunol. **16:**89–109.
23. **Levy, S., and T. Shoham.** 2005. The tetraspanin web modulates immune-signalling complexes. Nat. Rev. Immunol. **5:**136–148.
24. **Li, Q., A. L. Brass, A. Ng, Z. Hu, R. J. Xavier, T. J. Liang, and S. J. Elledge.** 2009. A genome-wide genetic screen for host factors required for hepatitis C virus propagation. Proc. Natl. Acad. Sci. U. S. A. **106:**16410–16415.
25. **Kato, T., T. Date, M. Miyamoto, A. Furusaka, K. Tokushige, M. Mizokami, and T. Wakita.** 2003. Efficient replication of the genotype 2a hepatitis C virus subgenomic replicon. Gastroenterology **125:**1808–1817.
26. **Koutsoudakis, G., E. Herrmann, S. Kallis, R. Bartenschlager, and T. Pietschmann.** 2007. The level of CD81 cell surface expression is a key determinant for productive entry of hepatitis C virus into host cells. J. Virol. **81:**588–598.
27. **Lanford, R. E., C. Sureau, J. R. Jacob, R. White, and T. R. Fuerst.** 1994. Demonstration of in vitro infection of chimpanzee hepatocytes with hepatitis C virus using strand-specific RT/PCR. Virology **202:**606–614.
28. **Lott, W. B., S. S. Takyar, J. Tuppen, D. H. Crawford, M. Harrison, T. P. Sloots, and E. J. Gowans.** 2001. Vitamin B12 and hepatitis C: molecular biology and human pathology. Proc. Natl. Acad. Sci. U. S. A. **98:**4916–4921.
29. **Meuleman, P., J. Hesselgesser, M. Paulson, T. Vanwolleghem, I. Desombere, H. Reiser, and G. Leroux-Roels.** 2008. Anti-CD81 antibodies can prevent a hepatitis C virus infection in vivo. Hepatology **48:**1761–1768.
30. **Molina, S., V. Castet, L. Pichard-Garcia, C. Wychowski, E. Meurs, J. M. Pascussi, C. Sureau, J. M. Fabre, A. Sacunha, D. Larrey, J. Dubuisson, J. Coste, J. McKeating, P. Maurel, and C. Fournier-Wirth.** 2008. Serum-derived hepatitis C virus infection of primary human hepatocytes is tetraspanin CD81 dependent. J. Virol. **82:**569–574.
31. **Moradpour, D., F. Penin, and C. M. Rice.** 2007. Replication of hepatitis C virus. Nat. Rev. Microbiol. **5:**453–463.
32. **Ng, T. I., H. Mo, T. Pilot-Matias, Y. He, G. Koev, P. Krishnan, R. Mondal, R. Pithawalla, W. He, T. Dekhtyar, J. Packer, M. Schurdak, and A. Molla.** 2007. Identification of host genes involved in hepatitis C virus replication by small interfering RNA technology. Hepatology **45:**1413–1421.
33. **Oren, R., S. Takahashi, C. Doss, R. Levy, and S. Levy.** 1990. TAPA-1, the target of an antiproliferative antibody, defines a new family of transmembrane proteins. Mol. Cell. Biol. **10:**4007–4015.
34. **Pileri, P., Y. Uematsu, S. Campagnoli, G. Galli, F. Falugi, R. Petracca, A. J. Weiner, M. Houghton, D. Rosa, G. Grandi, and S. Abrignani.** 1998. Binding of hepatitis C virus to CD81. Science **282:**938–941.
35. **Randall, G., M. Panis, J. D. Cooper, T. L. Tellinghuisen, K. E. Sukhodolets, S. Pfeffer, M. Landthaler, P. Landgraf, S. Kan, B. D. Lindenbach, M. Chien, D. B. Weir, J. J. Russo, J. Ju, M. J. Brownstein, R. Sheridan, C. Sander, M. Zavolan, T. Tuschl, and C. M. Rice.** 2007. Cellular cofactors affecting hepatitis C virus infection and replication. Proc. Natl. Acad. Sci. U. S. A. **104:**12884–12889.
36. **Reed, K. E., and C. M. Rice.** 2000. Overview of hepatitis C virus genome structure, polyprotein processing, and protein properties. Curr. Top. Microbiol. Immunol. **242:**55–84.
37. **Sabahi, A.** 2009. Hepatitis C virus entry: the early steps in the viral replication cycle. Virol. J. **6:**117.
38. **Sato, K., J. Aoki, N. Misawa, E. Daikoku, K. Sano, Y. Tanaka, and Y. Koyanagi.** 2008. Modulation of human immunodeficiency virus type 1 infectivity through incorporation of tetraspanin proteins. J. Virol. **82:**1021–1033.
39. **Silvie, O., E. Rubinstein, J. F. Franetich, M. Prenant, E. Belnoue, L. Rénia, L. Hannoun, W. Eling, S. Levy, C. Boucheix, and D. Mazier.** 2003. Hepatocyte CD81 is required for Plasmodium falciparum and Plasmodium yoelii sporozoite infectivity. Nat. Med. **9:**93–96.
40. **Song, Y., P. Friebe, E. Tzima, C. Jünemann, R. Bartenschlager, and M. Niepmann.** 2006. The hepatitis C virus RNA 3′-untranslated region strongly enhances translation directed by the internal ribosome entry site. J. Virol. **80:**11579–11588.
41. **Tai, A. W., Y. Benita, L. F. Peng, S. S. Kim, N. Sakamoto, R. J. Xavier, and R. T. Chung.** 2009. A functional genomic screen identifies cellular cofactors of hepatitis C virus replication. Cell Host Microbe **5:**298–307.
42. **Takeuchi, T., A. Katsume, T. Tanaka, A. Abe, K. Inoue, K. Tsukiyama-Kohara, R. Kawaguchi, S. Tanaka, and M. Kohara.** 1999. Real-time detection system for quantification of hepatitis C virus genome. Gastroenterology **116:**636–642.
43. **Tanabe, Y., N. Sakamoto, N. Enomoto, M. Kurosaki, E. Ueda, S. Maekawa, T. Yamashiro, M. Nakagawa, C. H. Chen, N. Kanazawa, S. Kakinuma, and M. Watanabe.** 2004. Synergistic inhibition of intracellular hepatitis C virus

replication by combination of ribavirin and interferon-alpha. J. Infect. Dis. **189:**1129–1139.

44. **Tardif, M. R., and M. J. Tremblay.** 2005. Tetraspanin CD81 provides a costimulatory signal resulting in increased human immunodeficiency virus type 1 gene expression in primary CD4+ T lymphocytes through NF-kappaB, NFAT, and AP-1 transduction pathways. J. Virol. **79:**4316–4328.
45. **Timpe, J. M., Z. Stamataki, A. Jennings, K. Hu, M. J. Farquhar, H. J. Harris, A. Schwarz, I. Desombere, G. L. Roels, P. Balfe, and J. A. McKeating.** 2008. Hepatitis C virus cell-cell transmission in hepatoma cells in the presence of neutralizing antibodies. Hepatology **47:**17–24.
46. **Wakita, T., T. Pietschmann, T. Kato, T. Date, M. Miyamoto, Z. Zhao, K. Murthy, A. Habermann, H. G. Kräusslich, M. Mizokami, R. Bartenschlager, and T. J. Liang.** 2005. Production of infectious hepatitis C virus in tissue culture from a cloned viral genome. Nat. Med. **11:**791–796.
47. **Witteveldt, J., M. J. Evans, J. Bitzegeio, G. Koutsoudakis, A. M. Owsianka, A. G. Angus, Z. Y. Keck, S. K. Foung, T. Pietschmann, C. M. Rice, and A. H. Patel.** 2009. CD81 is dispensable for hepatitis C virus cell-to-cell transmission in hepatoma cells. J. Gen. Virol. **90:**48–58.
48. **Yunta, M., and P. A. Lazo.** 2003. Tetraspanin proteins as organisers of membrane microdomains and signalling complexes. Cell. Signal. **15:**559–564.
49. **Zhang, J., G. Randall, A. Higginbottom, P. Monk, C. M. Rice, and J. A. McKeating.** 2004. CD81 is required for hepatitis C virus glycoprotein-mediated viral infection. J. Virol. **78:**1448–1455.
50. **Zhang, Y. Y., B. H. Zhang, D. Theele, S. Litwin, E. Toll, and J. Summers.** 2003. Single-cell analysis of covalently closed circular DNA copy numbers in a hepadnavirus-infected liver. Proc. Natl. Acad. Sci. U. S. A. **100:**12372–12377.
51. **Zhang, Y. Y., D. P. Theele, and J. Summers.** 2005. Age-related differences in amplification of covalently closed circular DNA at early times after duck hepatitis B virus infection of ducks. J. Virol. **79:**9896–9903.
52. **Zhong, J., P. Gastaminza, J. Chung, Z. Stamataki, M. Isogawa, G. Cheng, J. A. McKeating, and F. V. Chisari.** 2006. Persistent hepatitis C virus infection in vitro: coevolution of virus and host. J. Virol. **80:**11082–11093.

Yang et al. Virology Journal 2010, 7:212
http://www.virologyj.com/content/7/1/212

VIROLOGY JOURNAL

SHORT REPORT Open Access

Inhibitory effects on HAV IRES-mediated translation and replication by a combination of amantadine and interferon-alpha

Lingli Yang[1,4†], Tomoko Kiyohara[2†], Tatsuo Kanda[1*†], Fumio Imazeki[1], Keiichi Fujiwara[1], Verena Gauss-Müller[3], Koji Ishii[2], Takaji Wakita[2], Osamu Yokosuka[1]

Abstract

Hepatitis A virus (HAV) causes acute hepatitis and sometimes leads to fulminant hepatitis. Amantadine is a tricyclic symmetric amine that inhibits the replication of many DNA and RNA viruses. Amantadine was reported to suppress HAV replication, and the efficacy of amantadine was exhibited in its inhibition of the internal ribosomal entry site (IRES) activities of HAV. Interferon (IFN) also has an antiviral effect through the induction of IFN stimulated genes (ISG) and the degradation of viral RNA. To explore the mechanism of the suppression of HAV replication, we examined the effects of the combination of amantadine and IFN-alpha on HAV IRES-mediated translation, HAV replicon replication in human hepatoma cell lines, and HAV KRM003 genotype IIIB strain replication in African green monkey kidney cell GL37. IFN-alpha seems to have no additive effect on HAV IRES-mediated translation inhibition by amantadine. However, suppressions of HAV replicon and HAV replication were stronger with the combination than with amantadine alone. In conclusion, amantadine, in combination of IFN-alpha, might have a beneficial effect in some patients with acute hepatitis A.

Short report

Hepatitis A virus (HAV), a member of the family Picornaviridae, causes acute hepatitis and occasionally fulminant hepatitis, a life-threatening disease. As the broad epidemiological picture of hepatitis A changes, the public health importance of this disease is being increasingly recognized [1]. It is a significant cause of morbidity worldwide, although the mortality rate due to hepatitis A is low (improved intensive care and transplantation have contributed to a reduction in deaths). Improved sanitation and living standards mean that fewer countries remain highly endemic, but the risk of HAV infection is present in countries lacking HAV immunity or where the endemicity of hepatitis A is low or intermediate [1]. In such situations, these outbreaks can prove to be long and difficult to control. Vaccination and informing the general public about good hygienic measures are important for the prevention of HAV infection, but new therapeutic options are also desirable.

Amantadine, a tricyclic symmetric amine, inhibits HAV replication *in vitro* [2]. We previously reported that amantadine inhibits hepatitis A virus internal ribosomal entry site (IRES)-mediated translation in human hepatoma cells [2]. Interferons (IFNs) also exhibit antiviral effects against HAV infection [2,3]. In the present study, we examined the effects of amantadine with or without IFN-alpha, on HAV IRES activities, HAV subgenomic replicon replication and HAV replication *in vitro* as a proof of concept for the development of a more effective treatment to control HAV infection.

First, we evaluated the cytotoxicity of amantadine and IFN-alpha by 3-(4,5-dimethylthiazol-2-yl)-5-(3-carboxymethoxyphenyl)-2-(4-sulfophenyl)-2H-tetrazolium, inner salt (MTS) assay. Amantadine concentrations in a range of 1 - 125 μg/mL and those of 1 - 150 μg/mL for 12-h incubation were non-toxic for Huh7 cells and for HuhT7 cells, respectively (Figures 1A and 1B). Amantadine could be incubated for a short time, e.g., 12 h, with the cells, and then the dose of amantadine could be

* Correspondence: kandat-cib@umin.ac.jp
† Contributed equally
[1]Department of Medicine and Clinical Oncology, Graduate School of Medicine, Chiba University, 1-8-1 Inohana, Chuo-ku, Chiba 260-8670, Japan
Full list of author information is available at the end of the article

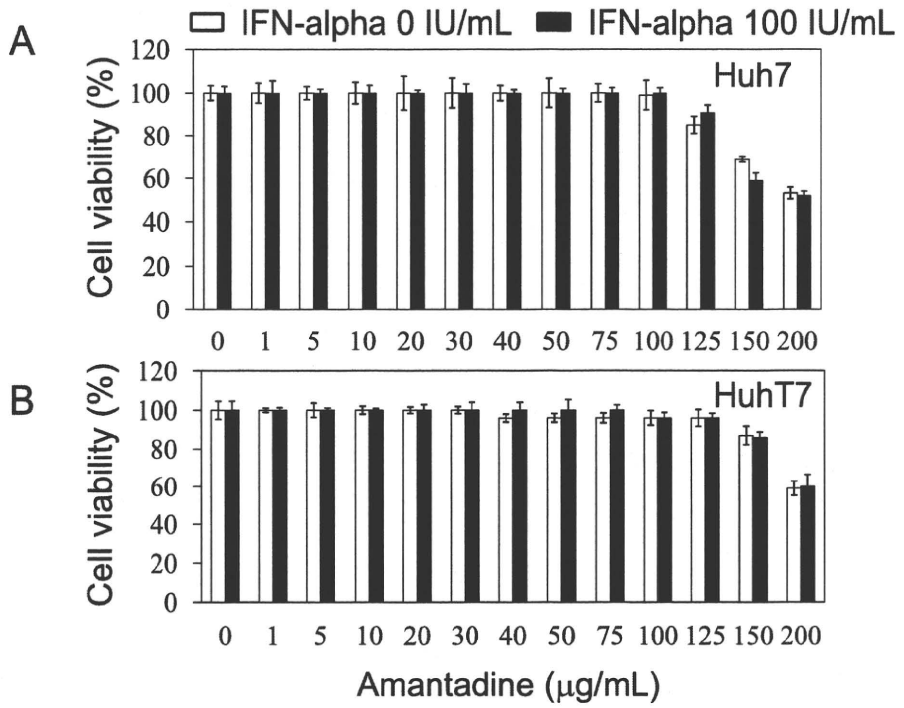

Figure 1 Effects of amantadine on cell growth and viability. MTS assays of cells 12 h after treatment with amantadine with or without 100 U/mL interferon (IFN)-alpha. (A) Huh7 cells. (B) HuhT7 cells. Data are expressed as mean ± SD.

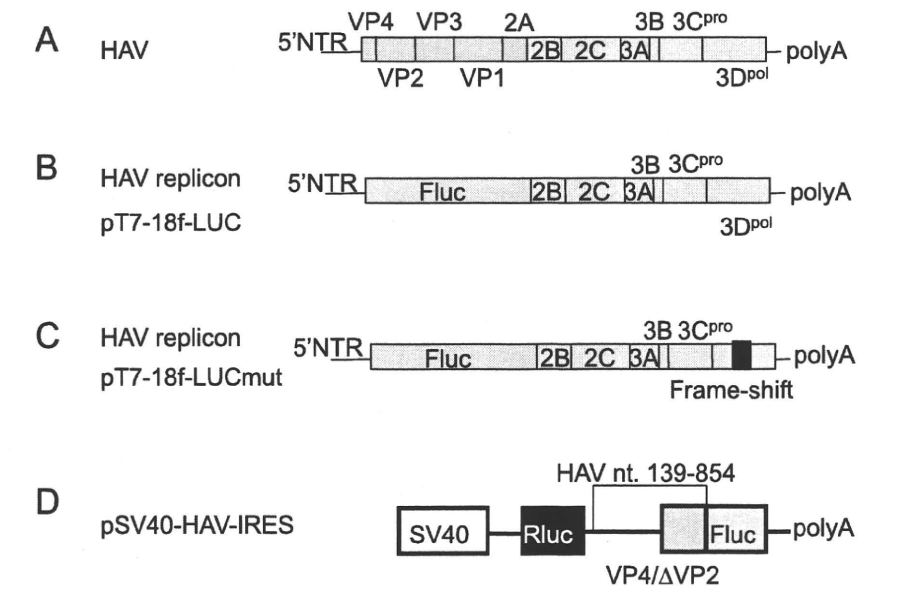

Figure 2 Structures of reporter constructs used in this study. (A) Structure of HAV genome. **(B)** Structure of the replication-competent HAV replicon (HAV replicon) pT7-18f-LUC, which contains an open-reading frame of firefly luciferase (Fluc) flanked by the first four amino acids of HAV polyprotein and by 12 C-terminal amino acids of VP1. This segment is followed by P2 and P3 domains of HAV polyprotein (HAV strain HM175 18f) [9,10]. **(C)** Structure of replication-incompetent HAV replicon (mut) (mut-HAV replicon) pT7-18f-LUCmut, which contains a frame-shift mutation in the polymerase 3 D [9,10]. **(D)** Bicistronic reporter constructs: pSV40-HAV IRES was described previously [2,4]. It encodes the Renilla luciferase genes (Rluc), the internal ribosomal entry site (IRES) HAV HM175, and the firefly luciferase gene (Fluc) under the control of the simian virus 40 promoter (SV40).

increased to higher than 100 μg/mL. With the combination of amantadine and 100 IU/mL IFN-alpha, we did not observe increased cytotoxicity compared with amantadine alone.

We previously reported that the introduction of siRNA targeted against the 5'NTR region of HAV HM175 inhibits HAV IRES-mediated translation and HAV replication [4]. Interestingly, amantadine and IFN also inhibited HAV IRES-mediated translation and HAV replication [2,3,5-8]. Accordingly, we planned to identify more effective strategies for suppressing HAV IRES-mediated translation and HAV replication. IRES is an attractive target for antivirals because HAV IRES is located in the 5'NTR region, the most conserved region among HAV strains. In the present study, we evaluated the HAV antiviral activity of amantadine and IFN-alpha. We initially examined the effects of this combination on HAV IRES-mediated translation using a luciferase reporter assay. Huh7 cells were transfected with pSV40-HAV IRES reporter vector, encoding SV40 promoter driven-*Renilla reniformis* and firefly luciferase, separated by HAV-IRES (Figure 2) [2], and treated with amantadine and/or IFN-alpha. Inhibition of luciferase activity at different levels was observed with amantadine with or without 100 IU/mL IFN-alpha (Figure 3A). Although the strongest suppression was noted with the combination of 10 μg/mL amantadine and 100 IU/mL IFN-alpha, IFN-alpha showed no additive effect on the translation inhibition by 50-100 μg/mL amantadine. This finding prompted us to examine whether IFN-alpha has additive suppression of HAV replicon replication by amantadine. We have reported that RNA replication of HAV can be analyzed in a DNA-based replicon system using HuhT7 cells that stably express T7-RNA polymerase in the cytoplasm (Figure 1) [9-11]. The luciferase activities determined after transfection of replicon DNA are a direct measure of RNA translation and replication. This is because replication in positive-stranded RNA viruses can be easily assessed with a viral replicon carrying the luciferase gene in place of viral structural genes. Moreover, luciferase activity due to translation or translation and replication can be evaluated when the transfection of a replication-competent replicon (HAV replicon) is compared with that of a replication-incompetent replicon (mut) (mut-HAV replicon) [8].

To further determine the effects of the combination of amantadine and IFN-alpha on HAV replication, we transfected the HAV replicon or mut-HAV replicon into HuhT7 cells, and the drugs were added 24 h later. Reporter assays were performed 48 or 72 h after transfection. The transfection efficacy of HAV replicon was estimated as 20-30% in our systems. Luciferase activity was normalized with respect to the protein concentration of cell

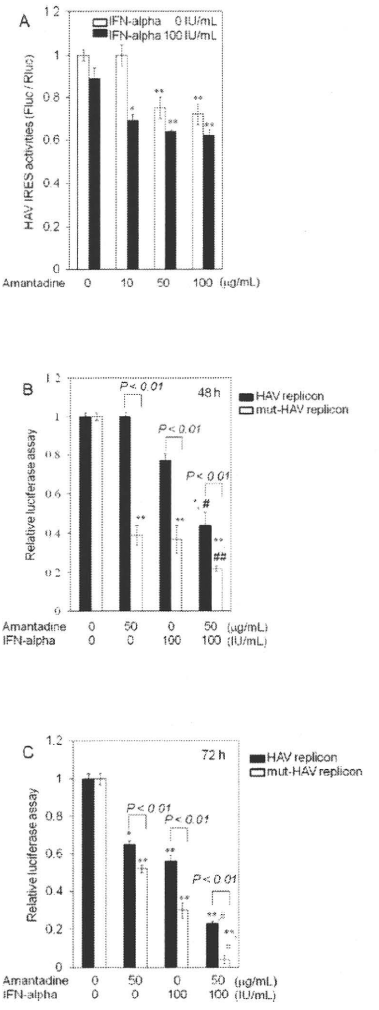

Figure 3 (A) Effects of amantadine with or without interferon on the hepatitis A virus (HAV) internal ribosomal entry site (IRES) activities in Huh7 cells. Approximately 2 × 10^5 cells were seeded on a 6-well tissue culture plate (Iwaki Glass, Tokyo, Japan) 24 h prior to transfection. pSV40-HAV-IRES (0.3 μg) was transfected into Huh7 cells using the Effectene transfection reagent (Qiagen, Tokyo, Japan). 24 h after transfection, amantadine and/or IFN in various concentrations was added to cells. 48 h after transfection, cell extracts were prepared, and luciferase assays were performed using the Dual Luciferase assay system (Toyo Ink, Tokyo, Japan) according to the manufacturer's instructions [2]. For controlling the variations in transcription, IRES activity was assessed by measuring the ratio of *Renilla* and firefly luciferases. All samples were run in triplicate. *Renilla* and firefly luciferase activities were measured as relative light units using a luminescencer (JNRII-AB-2300; ATTO, Tokyo, Japan). **(B, C) Effects of amantadine with or without interferon on the HAV subgenomic replicon replication in HuhT7 cells. (B)** 48 h after transfection and **(C)** 72 h after transfection. Black columns, replication-competent HAV replicon; white columns, replication-incompetent HAV replicon (mut). Relative luciferase activities without any treatments were set at 1. Data are expressed as mean (columns) ± SD (vertical lines). *$P < 0.05$ and **$P < 0.01$, compared with untreated control by Student's t test. #$P < 0.01$ and ## $P < 0.05$, compared with amantadine alone or IFN-alpha alone by Student's t test.

lysates. In this DNA-based system, 48 h after transfection, the replication rates of the HAV replicon were 100%, 77%, and 44% compared to those of control when treated with amantadine alone, IFN alone, and their combination, respectively (Figure 3B). On the other hand, since the mut-HAV replicon cannot replicate, the luciferase activity (39%, 37%, and 22% compared to those of control for the same test conditions, respectively) is due to translation of the viral RNA and not replication. Amantadine alone showed 52% at 72 h, higher than 37% at 48 h, supporting the notion that amantadine might suppress translation of the viral RNA. Suppression effects of these treatments were stronger in the mut-HAV replicon than in the HAV replicon. These findings support our observation of the suppression of HAV IRES-mediated translation by amantadine and IFN-alpha. Suppression effects at 48 h after transfection by the combination of amantadine and IFN-alpha against HAV replication were stronger than those by amantadine or IFN-alpha monotreatment. IFN-alpha was more effective than amantadine against the HAV replicon ($P = 0.0027$) (Figure 3B).

Seventy-two hours after transfection, the replication rates of the HAV replicon were 65%, 56%, and 23% compared to those of control when treated with amantadine alone, IFN-alpha alone, and their combination, respectively (Figure 3C). The replication rates of the mut-HAV replicon were 52%, 30%, and 4% of those of control, respectively. IFN-alpha was more effective than amantadine against the replication of HAV replicon or mut-HAV replicon ($P < 0.001$ or $P < 0.001$). Suppression effects of the combination of amantadine and IFN-alpha at 72 h post-transfection were stronger than those of amantadine or IFN-alpha monotreatment. Suppression effects of these treatments were stronger in the mut-HAV replicon than in the HAV replicon. Moreover, it is important to note that the effects of this combination were observed at earlier time points (Figure 3C).

Next, we performed an infectivity assay using the virus to investigate the effects of combination of amantadine and IFN-alpha on tissue culture-adapted HAV strain KRM003 (genotype IIIB, accession no. L20536) propagation in African green monkey kidney GL37 cells [12-14]. GL37 cell monolayers in 96-well culture plates were infected with HAV at a multiplicity of infection (MOI) of 5 or 50 for 1 h at 37°C in a CO_2 incubator. Without removing the inoculum, drug-containing media were added to appropriate wells. The final concentrations of amantadine, IFN-alpha, and their combination were 50 μg/ml, 100 IU/ml and 50 μg/ml of amantadine and 100 IU/ml of IFN-alpha, respectively. After incubation for 72 h, infected cells were evaluated with ELISA. Suppression of HAV replication by the combination of amantadine and IFN-alpha was stronger than those of amantadine alone, IFN-alpha alone, and untreated control (Figure 4).

IFNs are proteins induced by lymphocytes and other cells including hepatocytes in response to viruses such as HAV. In virus-infected cells, dsRNA activates antiviral interferon pathways and the production of IFN type I. The secreted IFN type I induces a positive feedback loop that results in the expression of interferon-stimulated genes (ISGs), including RNase L and protein kinase R (PKR) [15]. Our study supports the fact that the administration of IFN-alpha suppresses HAV replication through HAV IRES mediated-translation and other mechanisms and that, on the other hand, amantadine suppresses HAV replication mainly through HAV IRES mediated-translation.

There are several reports concerning HAV suppressing intracellular dsRNA-induced retinoic acid-inducible gene I (RIG-I)-mediated IFN regulatory factor 3 (IRF-3) activation to block induction of IFN [16,17]. Yang et al. reported that HAV proteins interact with mitochondrial antiviral signaling protein, an essential component of virus-activated signaling pathways that induce protective IFN responses [18]. However, in this study, the

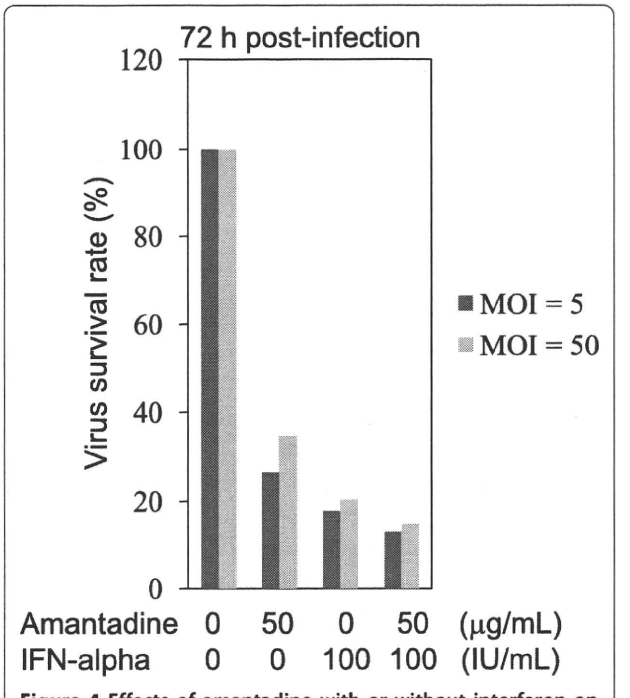

Figure 4 Effects of amantadine with or without interferon on HAV KRM003 genotype IIIB strain replication in African green monkey kidney cell GL37. GL37 cell monolayers in 96-well culture plates were infected with HAV [at a multiplicity of infection (MOI) of 5 or 40] for 1 h at 37°C in a CO_2 incubator. Amantadine and/or IFN was added to cells. After the incubation for 72 h, infected cells were evaluated with ELISA. The rate of virus survival was measured using this equation: Virus survival rate (%) = 100 × Absorbance with drug/Absorbance without drug.

administration of exogenous IFN-alpha could suppress HAV replication, although endogenous IFNs produced by cells also may play an important role in inhibiting viral replication. Further studies will be needed.

Amantadine inhibits the replication of many DNA and RNA viruses and is also used as a drug for the treatment of Parkinson's disease [2]. It is known that the M2 protein of influenza A virus is a target of amantadine [19]. Furthermore, it has been reported to inhibit HAV IRES-mediated translation and replication by our group and other researchers [2,3,5-8].

Therefore, we examined the possibilities of the combination of amantadine and IFN-alpha against HAV because these two drugs were previously reported to be effective against HAV [2,3,5-8]. To our knowledge, this is the first study demonstrating that a combination of amantadine and IFN-alpha can suppress HAV replication more effectively than amantadine or IFN-alpha alone.

Abbreviations

HAV: hepatitis A virus; **IRES**: internal ribosomal entry site; **IFN**: interferon; **MTS**: 3-(4,5-dimethylthiazol-2-yl)-5-(3-carboxymethoxyphenyl)-2-(4-sulfophenyl)-2H-tetrazolium, inner salt.

Acknowledgements

We thank Dr. S. U. Emerson for providing the plasmids. This work was supported by grants for Scientific Research 21590829, 21590828, and 21390225 from the Ministry of Education, Culture, Sports, Science, and Technology, Japan (TK, FI, and OY), a grant from the Ministry of Health, Labor, and Welfare of Japan (OY), and a grant from Chiba University Young Research-Oriented Faculty Member Development Program in Bioscience Areas (TK).

Author details

[1]Department of Medicine and Clinical Oncology, Graduate School of Medicine, Chiba University, 1-8-1 Inohana, Chuo-ku, Chiba 260-8670, Japan. [2]Department of Virology II, National Institute of Infectious Diseases, 4-7-1, Gakuen, Musashi-Murayama, Tokyo 280-0011, Japan. [3]Institute of Medical Molecular Biology, University of Lübeck, Ratzeburger Allee 160, D-23538 Lübeck, Germany. [4]Department of Dermatology, Graduate School of Medicine, Osaka University, Osaka 565-0871, Japan.

Authors' contributions

LY, Tatsuo Kanda, FI and OY conceived and designed the study. LY, Tomoko Kiyohara and Tatsuo Kanda performed the experiments. LY, Tomoko Kiyohara, Tatsuo Kanda and FI analyzed data and wrote the manuscript. Tomoko Kiyohara, KI and TW contributed to experiments using a whole HAV virus. Tomoko Kiyohara, Tatsuo Kanda and VG contributed to the interpretation of the interpretation of the results and took part to the critical revision of the manuscript. All authors read and approved the final manuscript.

Competing interests

The authors declare that they have no competing interests.

Received: 4 June 2010 Accepted: 3 September 2010
Published: 3 September 2010

References

1. FitzSimons D, Hendrickx G, Vorsters A, Damme PV: **Hepatitis A and E: update on prevention and epidemiology.** *Vaccine* 2010, **28**:583-588.
2. Kanda T, Yokosuka O, Imazeki F, Fujiwara K, Nagao K, Saisho H: **Amantadine inhibits hepatitis A virus internal ribosomal entry site-mediated translation in human hepatoma cells.** *Biochem Biophys Res Commun* 2005, **331**:621-629.
3. Widell A, Hansson BG, Oberg B, Nordenfelt E: **Influence of twenty potentially antiviral substances on in vitro multiplication of hepatitis A virus.** *Antiviral Res* 1986, **6**:103-112.
4. Kanda T, Zhang B, Kusov Y, Yokosuka O, Gauss-Müller V: **Suppression of hepatitis A virus genome translation and replication by siRNAs targeting the internal ribosomal entry site.** *Biochem Biophys Res Commun* 2005, **330**:1217-1223.
5. Kanda T, Imazeki F, Nakamoto S, Okitsu K, Yokosuka O: **Internal ribosomal entry-site activities of clinical isolates-derived hepatitis A virus and inhibitory effects of amantadine.** *Hepatol Res* 2010, **40**:415-423.
6. Crance JM, Biziagos E, Passagot J, van Cuyck-Gandre H, Deloince R: **Inhibition of hepatitis A virus replication in vitro by antiviral compounds.** *J Med Virol* 1990, **31**:155-160.
7. Chen Y, Zeng S, Hsu JTA, Horng J, Yang H, Shih S, Chu Y, Wu T: **Amantadine as a regulator of internal ribosome entry site.** *Acta Pharmacol Sin* 2008, **29**:1327-1333.
8. El-Sabbagh OI, Rady HM: **Synthesis of new acridines and hydrazones derived from cyclic b-diketone for cytotoxic and antiviral evaluation.** *Eur J Med Chem* 2009, **44**:3680-3686.
9. Gauss-Müller V, Kusov YY: **Replication of a hepatitis A virus replicon detected by genetic recombination in vivo.** *J Gen Virol* 2002, **83**:2183-2192.
10. Kanda T, Gauss-Müller V, Cordes S, Tamura R, Okitsu K, Wu S, Nakamoto S, Fujiwara K, Imazeki F, Yokosuka O: **Hepatitis A virus (HAV) proteinase 3C inhibits HAV IRES-dependent translation and cleaves the polypyrimidine tract-binding protein.** *J Viral Hepat* 2010, **17**:618-623.
11. Kanda T, Kusov Y, Yokosuka O, Gauss-Müller V: **Interference of hepatitis A virus replication by small interfering RNAs.** *Biochem Biophys Res Commun* 2004, **318**:341-345.
12. Robertson BH, Jansen RW, Khanna B, Totsuka A, Nainan OV, Siegl G, Widell A, Margolis HS, Isomura S, Ito K, Ishizu T, Moritsugu Y, Lemon SM: **Genetic relatedness of hepatitis A strains recovered from different geographical regions.** *J Gen Virol* 1992, **73**:1365-1377.
13. Totsuka A, Moritsugu Y: **Hepatitis A vaccine development in Japan.** In *Viral Hepatitis and Liver Disease.* Edited by: Nishioka K, Suzuki H, Mishiro S. Tokyo: Springer-Verlag; 1994:509-513.
14. Kiyohara T, Totsuka A, Yoneyama T, Ishii K, Ito T, Wakita T: **Characterization of anti-idotypic antibodies mimicking antibody- and receptor-binding sites on hepatitis A virus.** *Arch Virol* 2009, **154**:1263-1269.
15. Kanda T, Steele R, Ray R, Ray RB: **Hepatitis C virus infection induces the beta interferon signaling pathway in immortalized human hepatocytes.** *J Virol* 2007, **81**:12375-12381.
16. Fensterl V, Grotheer D, Berk I, Schlemminger S, Vallbracht A, Dotzauer A: **Hepatitis A virus suppresses RIG-I-mediated IRF-3 activation to block induction of beta interferon.** *J Virol* 2005, **79**:10968-10977.
17. Paulmann D, Magulski T, Schwarz R, Heitmann L, Flehming B, Vallbracht A, Dotzauer A: **Hepatitis A virus protein 2B suppresses beta interferon (IFN) gene transcription by interfering with IFN regulatory factor 3 activation.** *J Gen Virol* 2008, **89**:1593-1604.
18. Yang Y, Liang Y, Qu L, Chen Z, Yi M, Li K, Lemon SM: **Disruption of innate immunity due to mitochondrial targeting of a picornaviral protease precursor.** *Proc Natl Acad Sci USA* 2007, **104**:7253-7258.
19. Cady SD, Schmidt-Rohr K, Wang J, Soto CS, Degrado WF, Hong M: **Structure of the amantadine binding site of influenza M2 proton channels in lipid bilayers.** *Nature* 2010, **463**:689-692.

doi:10.1186/1743-422X-7-212
Cite this article as: Yang *et al.*: **Inhibitory effects on HAV IRES-mediated translation and replication by a combination of amantadine and interferon-alpha.** *Virology Journal* 2010 **7**:212.

Virus Research xxx (2011) xxx–xxx

Contents lists available at ScienceDirect

Virus Research

journal homepage: www.elsevier.com/locate/virusres

Short communication

An SV40 mutant defective in VP4 expression exhibits a temperature-sensitive growth defect

Shoichiro Tange, Takeshi Imai, Akira Nakanishi*

National Center for Geriatrics and Gerontology, Obu, Aichi 474-8522, Japan

ARTICLE INFO

Article history:
Received 14 October 2010
Received in revised form 1 February 2011
Accepted 1 February 2011
Available online xxx

Keywords:
Polyomavirus
SV40
Vp4
Temperature sensitive phenotype

ABSTRACT

On reexamination of temperature-sensitive D-type (tsD) mutants of simian virus 40 (SV40), we found that the tsD222 mutant is identical to the VP2 M228I mutant, which is defective in VP4 expression, at the nucleotide level. Although a previous study reported that lack of VP4 caused defects in viral dissemination in BSC-1 cells, this mutant showed a temperature-sensitive growth defect in CV-1 cells. tsD101:VP3 Q113K and tsD202:VP3 P108S exhibited a growth phenotype similar to that of tsD222, and they retained the VP4 open reading frame (ORF). These three mutants did not complement each other, suggesting that their defects were functionally indistinguishable. Transduction of the SV40 vector expressing wild-type VP4 in tsD222-infected cells did not ameliorate the growth defect at the non-permissive temperature. The results indicate that tsD mutation in minor capsid proteins has a more profound impact on viral propagation, and that lack of VP4 ORF seems to have little influence on viral growth.

Simian virus 40 (SV40), which belongs to the family *Polyomaviridae*, is a small DNA tumor virus with a circular, double-stranded DNA genome. Its capsid is composed of 360 VP1 major capsid proteins and approximately 72 VP2 and VP3 (VP2/3) minor capsid proteins. These two minor capsid proteins are encoded by the same mRNA and reading frame, but they differ in their translational start site; thus, VP2 is 118 residues longer than VP3. The open reading frame (ORF) for the minor capsid proteins harbors a small nonstructural protein, VP4, of approximately 15 kDa. The translational initiation site of VP4 is downstream of the VP3 initiation codon and it functions during viral lysis by facilitating the release of progeny virions (Daniels et al., 2007).

Minor capsid proteins are involved in the post-entry event during viral infection, i.e., during the intracellular trafficking and nuclear import of the viral genome (Nakanishi et al., 2006; Nakanishi et al., 2002). The original concept came from early studies of SV40 using temperature-sensitive D-type (tsD) SV40 mutants (Avila et al., 1976; Chou et al., 1974; Chou and Martin, 1974; Robb and Martin, 1972) in which mutations were physically mapped to the VP3 coding region between SV40 nucleotide number (SV40 nt) (Reddy et al., 1978) 1046 and 1493 (Lai and Nathans, 1975a; Lai and Nathans, 1975b; Shenk et al., 1975). These mutants were apparently defective in the uncoating process in which the initiation of viral gene expression on infection was blocked at the restrictive, non-permissive temperature, although their viral DNA was completely capable of initiating viral growth on transfection. We aimed to reexamine tsD mutants to determine whether such a phenotype could help us identify the domain that is important for viral uncoating, but instead we found that one of the tsD mutants is identical to that defective in VP4 expression.

Nucleotide alterations in tsD101, tsD202, and tsD222 (Chou and Martin, 1974; Robb and Martin, 1972) were identified as SV40 nt 1252C to A, 1237C to T, and 1245G to A, respectively (Fig. 1A) by sequencing the region encompassing VP3 coding region, from SV40 nt 900 to 1792, amplified with Herculase polymerase (Stratagene, La Jolla, CA), which has proofreading activity, using the respective mutant viral lysate as the template and the primers, 5′-ATATCAACAACCAGGAATGGCT-3′ and 5′-CAAAGGAATTCTAGCCACACTGTAGCA-3′. The amino acid changes were VP3 108 Pro to Ser (P108S) in tsD202, VP3 113 Gln to Lys (Q113K) in tsD101, and VP3 110 Met to Ile (M110I) in tsD222 (Fig. 1A). The mutations appeared to be clustered together on the amino-terminal side of the VP1-interactive domain of VP3 (Chen et al., 1998; Nakanishi et al., 2006), implying the presence of a functional domain. We note that nucleotide change in tsD222, VP3 M110I, is identical to that of VP2 M228I. This particular mutant is shown to be defective in VP4 expression and blocked in viral dissemination in BSC-1 cells (Daniels et al., 2007).

To confirm whether these mutations result in a temperature-sensitive phenotype, each individual nucleotide alteration as well as the combination of the three mutations, VP3 P108S-M110I-Q113K (PMQ/SIK), were introduced into an infectious molecular

* Corresponding author at: Section of Gene Therapy, Department of Aging Intervention, National Center for Geriatrics and Gerontology, 35 Gengo, Morioka, Obu, Aichi 474-8522, Japan. Tel.: +81 562 44 5651x5058; fax: +81 562 46 8461.
E-mail address: nakanish@ncgg.go.jp (A. Nakanishi).

0168-1702/$ – see front matter © 2011 Elsevier B.V. All rights reserved.
doi:10.1016/j.virusres.2011.02.001

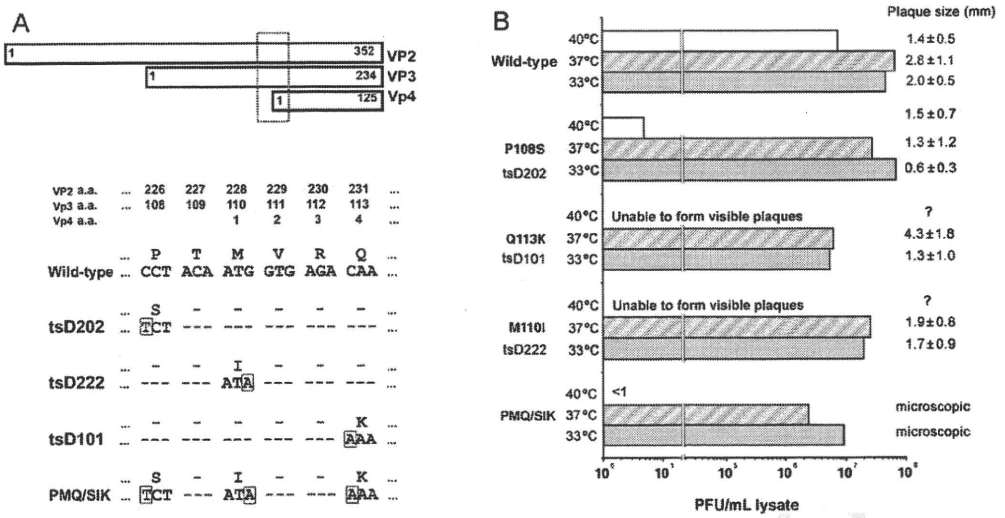

Fig. 1. Nucleotide alterations in SV40 tsD mutants resulting in temperature-sensitive phenotypes. (A) Nucleotide alterations in SV40 tsD mutants: The upper panel shows a schematic diagram of the VP2, VP3, and VP4 coding regions. The lower panel shows the nucleotide sequence of SV40 nt 1237 to 1254 encoding the partial open reading frame of the VP2, VP3, and VP4. The corresponding VP2, VP3, and VP4 amino acid numbers are indicated. Nucleotide alterations in tsD202, tsD222, tsD101, and PMQ/SIK are boxed and the resultant amino acid changes are shown. (B) Plaque assay of mutants introduced with the nucleotide alteration found in tsD mutants: Lysates of CV-1 cells transfected with the respective viral DNA were quantified for viral DNA using real-time quantitative PCR targeted to the SV40 origin sequence using SYBR Green Realtime PCR Master Mix Plus (Toyobo) and the primers, 5′-AAGCCTCCTCACTACTTCTGGAATAGCTC-3′ and 5′-AGCATGCATCTCAATTAGTCAGCAACCATA-3′, operated using LightCycler (Roche Applied Biosciences, Basel, Switzerland), and adjusted to contain 2.0×10^{11} viral DNA/mL as described (Nakanishi et al., 2008). The lysates were serially diluted, applied to CV-1 cells incubated at 40 °C (open column), 37 °C (shaded column), or 33 °C (dotted column), and stained for plaques (Nakanishi et al., 2002). Plaque-forming units (PFUs) present in the 1-mL cell lysate containing approximately 2.0×10^{11} viral DNA are shown as columns. Numbers shown at the side of the columns indicate mean plaque size ± standard deviation (mm).

clone of SV40, NOpSV40 SRBSM (Li et al., 2003), and pSV40, which harbors the natural SV40 genome, using *Sal*I and *Rsr*II and *Eco*RV and *Afl*II, respectively. Both types of viral DNA were excised by digestion with *Bam*HI and religated to generate infectious viral DNA (Ishii et al., 1994). Unless otherwise noted the results presented below are from experiments using viral DNA derived from NOpSV40. Upon DNA transfection into the CV-1 and BSC-1 cell lines, the extent of viral DNA replication and capsid protein expression at 72-h after transfection was similar among the mutants, including PMQ/SIK and the wild-type virus, irrespective of the cell type or temperature (40 °C or 37 °C) (Supplemental Fig. S1), which is consistent with previous results showing that DNA of tsD mutants were fully infectious (Chou and Martin, 1975; Daniels et al., 2007; Robb and Martin, 1972). Viral lysates, prepared by transfecting the respective viral DNA into CV-1 cells, were used to test viability of the viruses by infecting CV-1 cells in the plaque assay (Fig. 1B). At permissive temperatures (33 °C or 37 °C), all mutants except for PMQ/SIK produced similar number of plaques as that produced by the wild-type virus (Fig. 1B). PMQ/SIK produced very small plaques that were only discernable under a microscope. At restrictive temperatures (40 °C), all mutants were defective in plaque production, thereby confirming the temperature-sensitive phenotype of these mutants. At a high multiplicity of infection (MOI), infection with Q113K or M110I resulted in a cytopathic effect in most cells, although no visible plaques were present at lower MOIs (Supplemental Fig. S2). P108S produced 10^7-fold less plaques at 40 °C, and PMQ/SIK was nonviable at 40 °C.

When natural SV40 was used as the parental genome, the viability of the mutant harboring M110I or Q113K mutations at 40 °C was approximately 10^2-fold less than that at 33 °C (Supplemental Table S1), whereas approximately 10^3- to 10^4-fold less viability was observed in the previous study (Chou and Martin, 1974). We also noticed that NOSV40 grew more slowly than natural SV40, though the difference was not much pronounced (data not shown). Such minor growth delays might emphasize the mutant's phenotype, i.e., defective in growth at the non-permissive temperature or in BSC-1 cells (discussed below). Although the extent of decrease in viability varies among parental plasmids or experiments, M110I, Q113K, and P108S mutations apparently resulted in the temperature-sensitive phenotype in CV-1 cells (Fig. 1B).

Since the mutants were originally identified by their inability to initiate viral DNA replication on infection at non-permissive temperatures (Chou and Martin, 1975), they were examined at the onset of viral gene expression in CV-1 cells at 37 °C or 40 °C, as well as in BSC-1 cells at 37 °C. The experiments hereafter were performed at 37 °C, considering 37 °C as the permissive temperature because we consistently observed that viability at 33 °C and 37 °C was identical. Cell lysates containing viral particles were adjusted to contain 2.0×10^{11} copies of viral DNA/mL (see Fig. 1B legend) and were used for infecting the cells applying about thousand viral DNA to each cell. When examined for T antigen expression at 60-h after infection (hours post-infection, hpi) by Western blot, the T antigen signal was detected only in wild-type-infected CV-1 cells incubated at both temperatures (Fig. 2A, upper panel). A very faint signal was detected in Q113K-infected CV-1 cells incubated at 37 °C, while the signal in wild-type-infected BSC-1 cells and the remaining mutant-infected cells was undetectable. To employ a more sensitive approach, T antigen expression was detected by immunofluorescence staining of the infected cells (Fig. 2B). On infection with wild-type viruses, almost all cells became T antigen positive at 60 hpi, while mutant-infected cells exhibited a lower proportion of T antigen-positive cells, irrespective of cell type or temperature (Fig. 2B). M110I-infected cells exhibited approximately 50% positive cells, while Q113K-infected cells were 50–75% positive for T antigen expression. P108- and PMQ/SIK-infected cells showed a much lower proportion of T antigen-positive cells; approximately 25% for P108-infected cells and <10% for PMQ/SIK-infected cells. Notably, the signal in BSC-1 cells tended to be weak compared with that in CV-1 cells, which may explain why the Western blot signal from BSC-1 cells was much lower than that from CV-1 cells. Thus, all mutants exhibited defects in viral gene expression under all conditions examined, and these data were consistent

Please cite this article in press as: Tange, S., et al., An SV40 mutant defective in VP4 expression exhibits a temperature-sensitive growth defect. Virus Res. (2011), doi:10.1016/j.virusres.2011.02.001

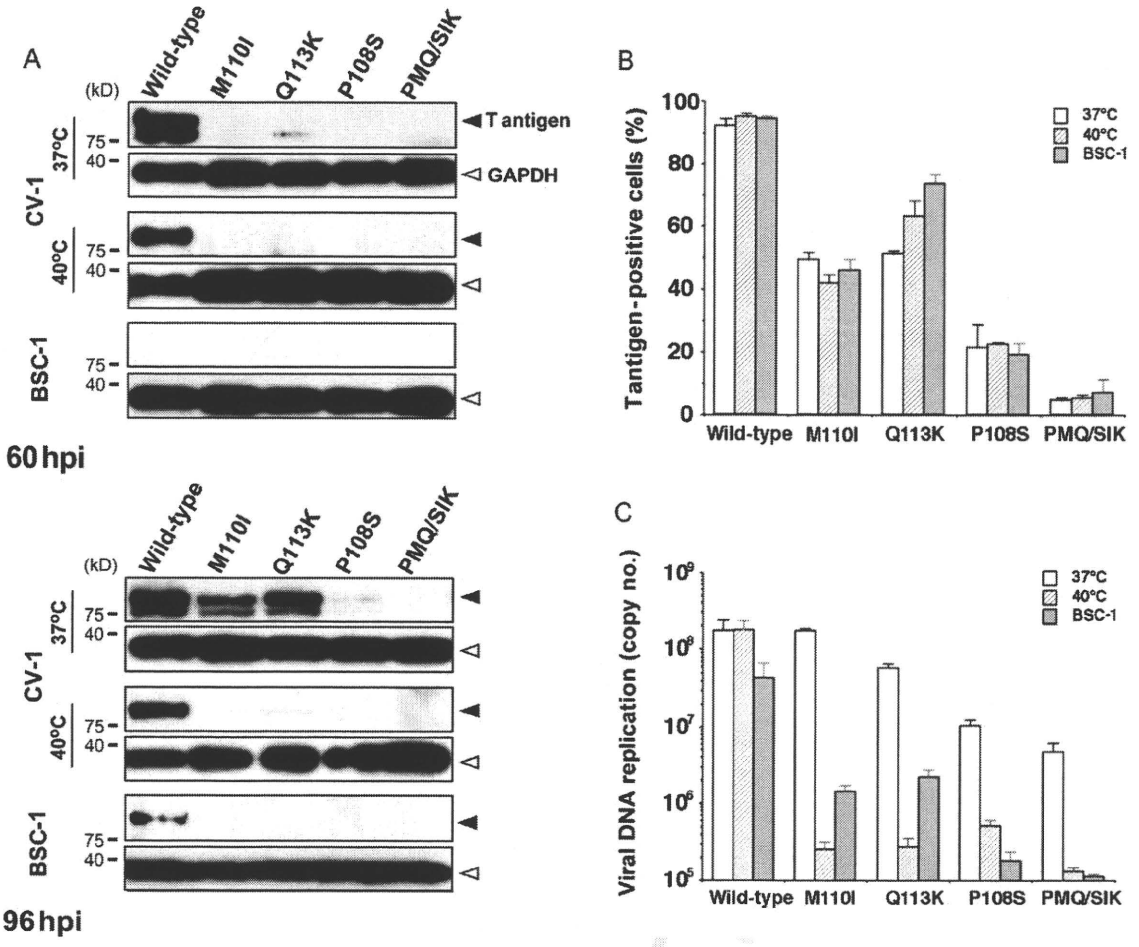

Fig. 2. Viral gene expression and viral DNA replication of mutants harboring tsD mutations. (A) Western blot detection of T antigen expression on infection with mutants: CV-1 or BSC-1 cells infected with either wild-type or the mutant were harvested for detecting the T antigen by Western blot at 60 h hpi (upper panel) or 96 hpi (lower panel). Approximately half of the cells harvested from individual six-well plates were used for detecting the SV40 T antigen using mouse monoclonal anti-T antigen (PAb419; Oncogene Sci., USA) as the primary antibody and peroxidase-conjugated anti-mouse IgG antibody (GE Healthcare, Bucks, UK) as the secondary antibody followed by enzyme chemiluminescence (ECL) (Immunostar; Wako chemicals, Osaka, Japan). As a loading control, glyceraldehyde-3-phosphate dehydrogenase (GAPDH) was detected using mouse anti-GAPDH antibody (clone 6C5; Millipore, Billerica, MA, USA) by ECL similar to the T antigen. Note that wild-type-infected cells tended to have lower amounts of protein because of an effective blockage of cell growth on infection, whereas the mutant-infected cells were less interfered with the growth likely due to lower incident of viral infection or lower level of viral gene expression. Positions of molecular weight markers for 75 and 45 kDa as well as those of the T antigen (filled arrowhead) and GAPDH (open arrowhead) are indicated. (B) Immunofluorescence detection of T antigen expression on infection: Cell lysates containing viral particles, adjusted for viral DNA as in the plaque assay (Fig. 1B), were used to infect CV-1 cells incubated at 37 °C (open columns) or 40 °C (shaded columns), and to BSC-1 cells incubated at 37 °C (closed columns). At 60 hpi, the cells were fixed, and the proportion of T antigen-positive cells were examined by immunocytochemistry using mouse monoclonal anti-T antigen antibody and Alexa Fluor 488-conjugated goat anti-mouse IgG antibody (Molecular probes, Eugene, OR, USA). (C) Viral DNA replication on infection with mutants: The cells infected as described in Fig. 2B were extracted for low molecular weight DNA at 96 hpi as described (Nakanishi et al., 2006). The extracted DNA was quantified for SV40 DNA as described in Fig. 1B. The columns are designated as shown in Fig. 2B. The amount of viral DNA shown is the mean value of the triplicate with standard deviation as indicated.

with those obtained by Western blot detection of T antigen expression (Fig. 2A, upper panel).

When T antigen expression was examined for the lysate obtained at 96 hpi by Western blot, the comparable signal was detected in wild-type-, M110I-, and Q113K-infected CV-1 cells grown at permissive temperature. The lysate from wild-type-infected CV-1 cells grown at 40 °C and BSC-1 cells at 37 °C also contained detectable T antigen, while the signal was mostly undetected in mutant-infected CV-1 cells grown at 40 °C and in BSC-1 cells. Similarly, the extent of viral DNA replication examined by quantitative PCR showed that the levels of viral DNA in M110I- and Q113K-infected CV-1 cells grown at 37 °C were comparable with those in wild-type-infected cells, while a much lower extent of DNA replication was observed when the cells were incubated at 40 °C or in BSC-1 cells infected with the respective mutants (Fig. 2C). The growth of the mutants P108S and PMQ/SIK was affected by the mutation in CV-1 cells even grown at 37 °C and severely blocked at 40 °C and in BSC-1 cells. We note that viral growth in mutant-infected BSC-1 cells was similar to that in mutant-infected CV-1 cells at non-permissive temperature. Viral DNA replication in BSC-1 cells is known to be initiated 10–20 h later than that in CV-1 cells (Ritzi and Levine, 1970). Such slower viral growth in BSC-1 cells could make the mutants' growth defect more apparent similar to that in CV-1 cells grown at 40 °C. These results indicated that, similar to the previous observations using the mutants with natural SV40 backbone, the mutants showed growth defect in CV-1 cells at non-permissive temperature and in BSC-1 cells. P108S mutation appeared to affect viral gene expression and DNA replication more severely than M110I and Q113K mutations.

The VP4 ORF status differs among the mutants. tsD101 (Q113K) harbors the VP4 Gln 4 to Lys alteration, and tsD222 (M110I) harbors no VP4 ORF because of alteration in the initiation codon, whereas the tsD202 (P108S) VP4 ORF is unaffected by the mutation (Fig. 1). Chou and Martin (1974) showed that coinfection of

Please cite this article in press as: Tange, S., et al., An SV40 mutant defective in VP4 expression exhibits a temperature-sensitive growth defect. Virus Res. (2011), doi:10.1016/j.virusres.2011.02.001

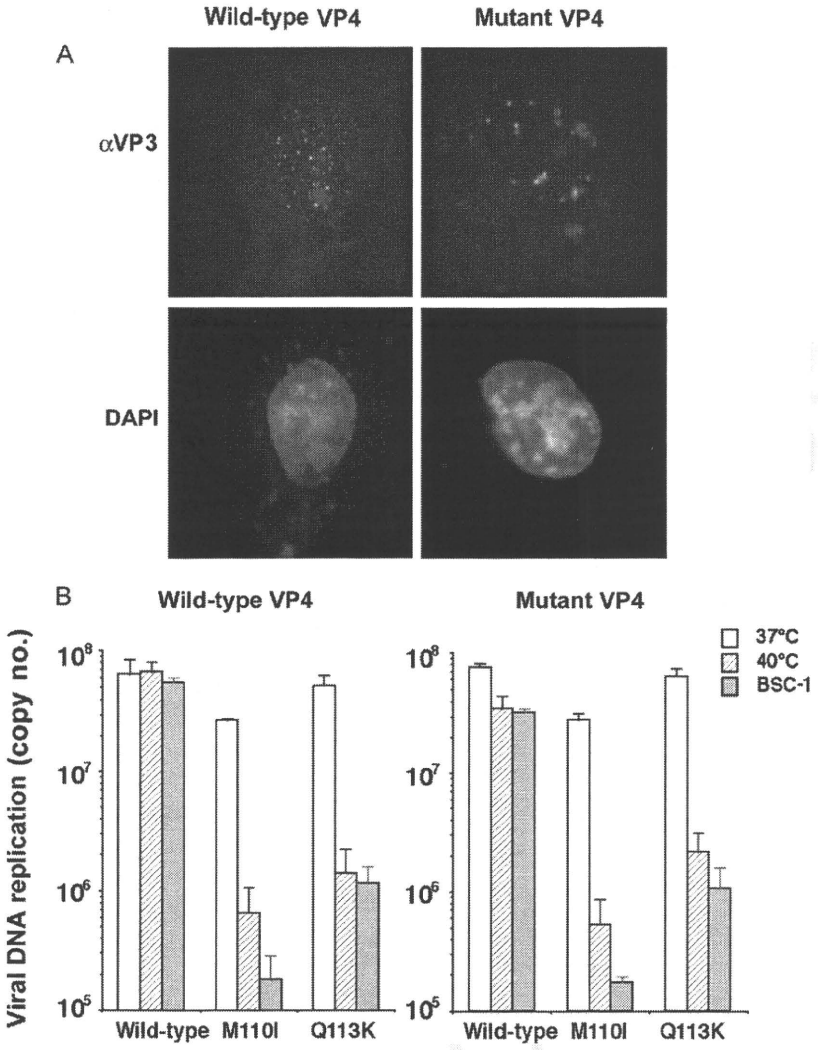

Fig. 3. VP4 complementation to mutant-infected cells. (A) Immunofluorescence detection of VP4 expressed from the VP4 expression vector: BSC-1 cells grown on coverslip were transfected with pSCMV VP4w or pSCMV VP4q using Lipofectamine 2000 (Invitrogen, Carlsbad, CA, USA) following the manufacturer's instruction. Cells were fixed at 48-h after transfection with acetone–methanol and stained for VP4 using rabbit anti-VP3 antibody (Abcam, Cambridge, UK) followed by Alexa Fluor 555-conjugated goat anti-rabbit IgG antibody (Molecular probes, Eugene, OR, USA). 4′,6-diamidino-2-phenylindole (DAPI) was used to counterstain for visualizing the cell nucleus. Identical set of cells showing representative images observed under the epifluorescent microscope are shown. (B) Viral DNA replication on VP4 complementation: CV-1 or BSC-1 cells grown in six-well plates were applied with approximately 1000 viral particles and approximately 1000 SV40 vectors carrying the VP4 expression vector to each cell. Viral DNA found in the cells coinfected with the vector carrying either pSCMV VP4w (left panel: Wild-type VP4) or pSCMV VP4q (right panel: Mutant VP4) incubated at designated temperature at 96 hpi was quantified for viral DNA as shown in Fig. 1B. The columns are marked as shown in Fig. 2B.

tsD202 and tsD222 or tsD101 at the non-permissive temperature did not complement the plaque forming-activity, showing that each pair of mutants harbor a genetically indistinguishable defect. Similarly, coinfection of CV-1 cells with Q113K and M110I with a natural SV40 backbone at 40 °C did not change their plaque-forming activity, confirming that the mutants belong to the same complementation group and their defects are genetically indistinguishable (Supplemental Table S1). When the mutations were combined, exemplified in the PMQ/SIK mutant, growth was more severely affected than those in the original mutants (Fig. 1B), suggesting that the gathered mutations had a cumulative impact on viral growth.

We examined by Western blot the presence or absence of VP4 in CV-1 and BSC-1 cells infected with their respective mutants. However, multiple attempts to detect VP4 using an antibody similar to that used in the original report (Daniels et al., 2007) (and provided by the same source) as well as a commercially available antibody (Anti-VP2/3; Abcam, Cambridge, UK) were unsuccessful. The VP3 proteins appeared to be highly prone to partial digestion in the cell, and proteins smaller than VP3 (approximately 25, 18, 16, and 12 kDa) that were reactive to the antibody were frequently detected in the virus-infected cells, causing difficulty in identifying the VP4 band (data not shown). We also examined VP4 ORF by *in vitro* translation using the PCR fragments harboring the VP3 coding region of either wild-type's or the mutants'. We did find VP4-like band, though very faint, that appeared in the *in vitro* translation of the wild-type VP3 coding region but not in those harboring M110I mutation (Supplemental Fig. S3). Instead of pursuing VP4 detection, we examined whether lack of VP4 is the cause of the growth defect at non-permissive temperatures in CV-1 cells or of the reduced infectivity in BSC-1 cells, i.e., whether supplying VP4 to mutant-infected cells would restore viral growth. To this end, we made the VP4 expression vectors pSCMV VP4w and pSCMV VP4q carrying wild-type VP4 ORF and VP4 ORF with VP3 Q113K (VP4 Q4K) mutation, respectively. Briefly, the ZsGreen coding region of pSCMV-ZG (Nakanishi

Please cite this article in press as: Tange, S., et al., An SV40 mutant defective in VP4 expression exhibits a temperature-sensitive growth defect. Virus Res. (2011), doi:10.1016/j.virusres.2011.02.001

et al., 2008) was replaced with that of VP4 ORFs amplified by PCR using NOpSV40 or NOpSV40 Q113K as the template and the primers

5′-GGCCCGGGATCCACCGGTCGCCACCATGGTGAGACAAGTAGCC-3′

and 5′-TCTAGAGGGTCGTGTACATTAACTC-3′ (restriction sites are underlined) using the *AgeI* and *BsrGI* sites. The constructs harbor the human cytomegalovirus immediate-early promoter and SV40 origin that drives expression of VP4, introduced with a strong ATG context (boxed sequence in the primer) for ensuring VP4 translation, and are also available for packaging to the SV40 vector because of the presence of the SV40 origin (Nakanishi et al., 2008). On transfection of the constructs into BSC-1 cells followed by immunofluorescence detection of VP4 using anti-VP3 antibody, positive signals seen as nuclear dots, similar to those reported previously (Daniels et al., 2007), were evident (Fig. 3A). SV40 vectors packaging pSCMV VP4w or VP4q were then made by cotransfection of 293T cells with pCAG SV40, pCI Ts, and either pSCMV VP4w or VP4q, purified for the SV40 vector by 27–39% Optiprep gradient sedimentation (Nakanishi et al., 2008). The vectors were transduced into CV-1 or BSC-1 cells and coinfected with the viral particles either of wild-type, M110I, or Q113K. The cells were then examined for the extent of viral DNA replication at 96 hpi using quantitative real-time PCR (Fig. 3B). On coinfection with the VP4 vector expressing wild-type or mutant VP4, the extent of viral DNA replication did not recover in mutant-infected CV-1 cells incubated at non-permissive temperature as well as in mutant-infected BSC-1 cells; the profile of viral growth defect was unchanged with or without wild-type VP4 transduction by the VP4 expression vector. The results suggested that presence of wild-type or mutant VP4 did not complement the growth defect of the mutants and was consistent with the idea that these growth defects occur in the early stages of infection.

Here we report that the tsD222 mutant is identical to VP2 M228I, known to be defective in expressing VP4 (Daniels et al., 2007), though the mutant showed a conditional temperature growth phenotype in CV-1 cells. Genetic complementation studies confirmed that the growth defect was not related to the absence of an intact VP4 ORF, since the growth of tsD101 (Q113K), in which VP4's fourth amino acid was altered from Gln to Lys, and tsD202 (P108S), in which VP4 ORF was intact, was also affected, and they did not genetically complement each other. The mutants in the context of a natural genome as well as in the context of an NOSV40 viral genome, in which the overlapping coding regions of VP2/3 and VP1 are separated by a duplication of the overlapping region, exhibited similar phenotypes with a temperature-sensitive growth defect in CV-1 cells and the inability to genetically complement each other (Supplemental Table S1 and data not shown). Consistent with these results, supplying VP4 *in trans* using the VP4 expression vector did not ameliorate the mutants' growth at non-permissive temperatures and in BSC-1 cells (Fig. 3). Since viral gene expression and DNA replication were affected by the mutations, our results indicated that the defect in the mutants involves one or more defects in VP2/3. This is reasonable given that VP4 is a nonstructural protein that is expressed in the very late stage of infection and thus mediating viral spread, which is the major role of VP4 (Daniels et al., 2007). Thus, the effect of tsD mutation is more significant in the early stages of viral infection during viral propagation, and a defect in mutant VP2/3 made a more significant contribution to the temperature-sensitive phenotype than the absence of a functional VP4.

Acknowledgments

We thank Dr. Ariella Oppenheim (Hebrew University) for the generous gift of anti-VP3 anti-serum, and Dr. Harumi Kasamatsu (University of California, Los Angeles) and Dr. Mary J. Tevethia .(Pennsylvania tsD222 This work was supported by a Grant- State University) for providing the viral lysates of tsD101, tsD202, and in-Aid for Scientific Research from Japan Society for the Promotion of Science and Health Labor Sciences Research Grant on "Research on Emerging and Re-emerging Infectious Diseases" to AN.

Appendix A. Supplementary data

Supplementary data associated with this article can be found, in the online version, at doi:10.1016/j.virusres.2011.02.001.

References

Avila, J., Saral, R., Martin, R.G., Khoury, G., 1976. The temperature-sensitive defect in SV40 group D mutants. Virology 73 (1), 89–95.
Chen, X.S., Stehle, T., Harrison, S.C., 1998. Interaction of polyomavirus internal protein VP2 with the major capsid protein VP1 and implications for participation of VP2 in viral entry. EMBO J. 17 (12), 3233–3240.
Chou, J.Y., Avila, J., Martin, R.G., 1974. Viral DNA synthesis in cells infected by temperature-sensitive mutants of simian virus 40. J. Virol. 14 (1), 116–124.
Chou, J.Y., Martin, R.G., 1974. Complementation analysis of simian virus 40 mutants. J. Virol. 13 (5), 1101–1109.
Chou, J.Y., Martin, R.G., 1975. DNA infectivity and the induction of host DNA synthesis with temperature-sensitive mutants of simian virus 40. J. Virol. 15 (1), 145–150.
Daniels, R., Sadowicz, D., Hebert, D.N., 2007. A very late viral protein triggers the lytic release of SV40. PLoS Pathog. 3 (7), e98.
Ishii, N., Nakanishi, A., Yamada, M., Macalalad, M.H., Kasamatsu, H., 1994. Functional complementation of nuclear targeting-defective mutants of simian virus 40 structural proteins. J. Virol. 68 (12), 8209–8216.
Lai, C.J., Nathans, D., 1975a. A map of temperature-sensitive mutants of simian virus 40. Virology 66 (1), 70–81.
Lai, C.J., Nathans, D., 1975b. Mapping the genes of simian virus 40. Cold. Spring. Harb. Sympos. Quant. Biol. 39 (Pt. 1), 53–60.
Li, P.P., Naknanishi, A., Tran, M.A., Ishizu, K., Kawano, M., Phillips, M., Handa, H., Liddington, R.C., Kasamatsu, H., 2003. Importance of Vp1 calcium-binding residues in assembly, cell entry, and nuclear entry of simian virus 40. J. Virol. 77 (13), 7527–7538.
Nakanishi, A., Chapellier, B., Maekawa, N., Hiramoto, M., Kuge, T., Takahashi, R.U., Handa, H., Imai, T., 2008. SV40 vectors carrying minimal sequence of viral origin with exchangeable capsids. Virology 379 (1), 110–117.
Nakanishi, A., Nakamura, A., Liddington, R., Kasamatsu, H., 2006. Identification of amino acid residues within simian virus 40 capsid proteins Vp1, Vp2, and Vp3 that are required for their interaction and for viral infection. J. Virol. 80 (18), 8891–8898.
Nakanishi, A., Shum, D., Morioka, H., Otsuka, E., Kasamatsu, H., 2002. Interaction of the Vp3 nuclear localization signal with the importin alpha 2/beta heterodimer directs nuclear entry of infecting simian virus 40. J. Virol. 76 (18), 9368–9377.
Reddy, V.B., Thimmappaya, B., Dhar, R., Subramanian, K.N., Zain, B.S., Pan, J., Ghosh, P.K., Celma, M.L., Weissman, S.M., 1978. The genome of simian virus 40. Science 200 (4341), 494–502.
Ritzi, E., Levine, A.J., 1970. Deoxyribonucleic acid replication in simian virus 40-infected cells. III. Comparison of simian virus 40 lytic infection in three different monkey kidney cell lines. J. Virol. 5 (6), 686–692.
Robb, J.A., Martin, R.G., 1972. Genetic analysis of simian virus 40.3. Characterization of a temperature-sensitive mutant blocked at an early stage of productive infection in monkey cells. J. Virol. 9 (6), 956–968.
Shenk, T.E., Rhodes, C., Rigby, P.W., Berg, P., 1975. Mapping of mutational alterations in DNA with S1 nuclease: the location of deletions, insertions and temperature-sensitive mutations in SV40. Cold. Spring. Harb. Symp. Quant. Biol. 39 (Pt. 1), 61–67.

ARTICLE IN PRESS

YVIRO-06066; No. of pages: 9; 4C:

Virology xxx (2011) xxx–xxx

Contents lists available at ScienceDirect

Virology

journal homepage: www.elsevier.com/locate/yviro

Novel DNA virus isolated from samples showing endothelial cell necrosis in the Japanese eel, *Anguilla japonica*

Tetsuya Mizutani [a,*,1], Yusuke Sayama [a,b,1], Akira Nakanishi [c,1], Hideharu Ochiai [d], Kouji Sakai [e], Kouji Wakabayashi [f], Nozomi Tanaka [f], Emi Miura [f], Mami Oba [a], Ichiro Kurane [a], Masayuki Saijo [a], Shigeru Morikawa [a], Shin-ich Ono [f,*]

[a] *Virology 1, National Institute of Infectious Diseases, Gakuen 4-7-1, Musashimurayama, Tokyo 208-0011, Japan*
[b] *Department of Virology, Tohoku University School of Medicine, 2-1 Seiryo-machi, Aoba-ku, Sendai 980-8575, Japan*
[c] *National Institute for Longevity Sciences, National Center for Geriatrics and Gerontology, 36-3 Gengo, Morioka-machi, Obu, Aichi 474-8522, Japan*
[d] *Research Institute of Biosciences, Azabu University, Fuchinobe 1-17-71, Chuo-ku, Sagamihara, Kanagawa 252-5201, Japan*
[e] *Division of Experimental Animals Research, National Institute of Infectious Diseases, 4-7-1 Gakuen, Musashi-Murayama, Tokyo 208-0011, Japan*
[f] *School of Marine Science and Technology, Tokai University, 3-20-1 Orido, Shimizu-ku, Shizuoka 424-8610, Japan*

ARTICLE INFO

Article history:
Received 19 October 2010
Returned to author for revision
6 December 2010
Accepted 28 December 2010
Available online xxxx

Keywords:
Novel DNA virus
Japanese eel endothelial cells-infecting virus
Anguilla japonica

ABSTRACT

Economic loss due to viral endothelial cell necrosis of eel (VECNE) of *Anguilla japonica* is a serious problem for the cultured Japanese eel market. However, the viral genome responsible for VECNE is unknown. We recently developed a rapid determination system for viral nucleic acid sequences (RDV) to determine viral genome sequences. In this study, viral DNA fragments were obtained using RDV, and approximately 15-kbp circular full genome sequences were determined using a next-generation sequencing system, overlapping PCR, and Southern blot analysis. One open reading frame (ORF) was homologous to the large T-antigen of polyomavirus; other ORFs have no homology with any nucleic or amino acid sequences of polyomavirus. Therefore, as this DNA virus might comprise a novel virus family, we provisionally named it Japanese eel endothelial cells-infecting virus (JEECV). JEECV was detected in both naturally and experimentally infected eels, suggesting that JEECV potentially causes VECNE.

Introduction

The Japanese eel *Anguilla japonica* is an important fish species in several Asian countries including Japan. Viral endothelial cell necrosis of eel (VECNE) of *A. japonica* is a serious problem in Japanese aquaculture industry (Egusa et al, 1989; Inoue et al, 1994; Ono and Nagai, 1997). In Shizuoka, a prefecture where the eel is mass-produced, the total production of Japanese eel was approximately 1700 tons (4 billion yen), and 107 tons worth of eel died from illness in 2008. Of these 107, 31 tons worth of the eels died from VECNE. Every year, 30–40% of the eels die from VECNE. Thus, economic loss due to VECNE is a serious problem in the cultured eel business. To prevent the spread of VECNE, obtaining genomic information of the unknown viral agent is crucial for developing a detection system and vaccines.

We and other groups reported that VECNE occurs naturally (Egusa et al, 1989; Inoue et al, 1994; Ono and Nagai, 1997). Naturally VECNE shows reddening of fins with a swollen abdomen. Intense congestion occurs in the gills, liver, and intestine. Histopathology of VECNE is characterized by intense congestion in the central venous sinuses of the gill filaments compared to healthy eels. This pathological change is accompanied by degeneration of nuclei of endothelial cell in blood vessels; this degeneration is characterized by swelling. Hexagonal virus particles measuring about 75 nm in diameter were observed in the nuclei. Thus, VECNE results from a systemic viral infection that causes necrosis of endothelial cells in blood vessels. VECNE was experimentally induced by injecting a filtered homogenized solution of diseased eels into the abdominal cavities of healthy eels (Ono and Nagai, 1997). Since the first report regarding VECNE was published in 1989 (Egusa et al, 1989), the causative virus has not been identified because cell culture systems for viral isolation are not available. Therefore, we established a cell line that originated from vascular endothelial cells of *A. japonica* (Ono et al, 2007). The primary Japanese eel endothelial (JEE) cell culture system was established using the dorsal aorta and aortic bulbs of healthy eels. To isolate the causative virus, gill lamellae were homogenized and centrifuged. The supernatant was then filtered using a 0.45-μm filter. The filtrate was added to JEE cells. At 7 days post-inoculation (p.i.), cytopathic effect (CPE) with markedly hypertrophied nuclei was observed (Ono et al, 2007). After a second passage, CPE was observed at 4 days p.i. Serial passages of the virus in JEE cells also induced CPE. When JEE cells were treated with 5-iodo-2′-deoxyuridine before virus inoculation, CPE was inhibited, strongly suggesting that the virus has DNA as its genome. In addition, this virus exhibited chloroform

* Corresponding authors. Mizutani is to be contacted at Fax: +81 425 65 3315.
E-mail address: tmizutan@nih.go.jp (T. Mizutani).
[1] These authors contributed equally to this study.

0042-6822/$ – see front matter © 2011 Elsevier Inc. All rights reserved.
doi:10.1016/j.virol.2010.12.057

resistance, suggesting it is not an envelope virus. The shape of this virus in JEE cells is the same as that in naturally infected eels, as confirmed by electron microscopy (EM). The isolated virus caused VECNE in eels, as determined by a previous study (Ono et al, 2007). Although this virus was believed to be an adenovirus-like virus from these data, nucleic acid sequences were not determined.

We recently developed a rapid determination system for viral nucleic acid sequences (called RDV) to determine viral genomic sequences without cloning in a plasmid vector (Mizutani et al, 2007). RDV allows for exhaustive identification of viruses compared to previous virus detection systems, such as RT-PCR, because it does not require specific primers for target virus nucleotide sequences. In previous studies, we identified several novel viruses, such as Ryukyu virus 1 (bat adenovirus) (Maeda et al, 2008), *Hipposideros diadema* herpesvirus 1 (from bat) (Watanabe et al, 2009), Bat betaherpesvirus 2 (Watanabe et al., in press), Ostrich virus 1 (orthoreovirus) (Sakai et al, 2009) and Phasi Charoen virus (mosquito bunyavirus) (Yamao et al, 2009). In this study, we used RDV with the supernatant of virus-infected JEE cells to obtain viral genomic sequences of the viruses infecting JEE cells.

Results

Virus shape in virus stock analyzed using EM

To confirm that the virus stocks (supernatant of virus-infected cells) cause VECNE in eels, 70th-passage virus stock was used in this study. Virus shapes were observed in the nuclei using electron microscopy (EM) (Fig. 1A and B) after JEE cells were infected with the virus stock. After filtering the virus stock using 0.45-μm filters, the virus was inoculated into eels. EM photographs of the gill are illustrated in Fig. 1C and D. Intense congestion occurred in the gill (Fig. 1E) and liver (Fig. 1F) at 8 days p.i. Although we evaluated a number of EM photographs of JEE cells and gills, we found only one species based on virus shape. This suggests that the virus stock over 70 passages in JEE cells contain agent(s) causing VECNE.

Partial viral genomic DNA sequences using RDV

To obtain viral DNA genomic sequences, DNA was extracted from the supernatant of virus-infected JEE cells at 4 days p.i. after RNase A and DNase I treatment. RDV was then performed. A total of 29 PCR products were extracted from agarose gels at the final step of RDV, and direct sequencing was performed. The nucleotide sequences were used to determine homologous sequences using BLASTx and tBLAST at the National Center for Biotechnology Information (NCBI) web site. Nine read sequences were not homologous to any genes. PCR primers were designed based on these sequences, and three read sequences (read-024, -004A, and -004C) were amplified in virus-infected cells, but not in mock-infected cells, using DNA samples (Fig. 2A). One read sequence, read-024, comprising 100 amino acids were homologous to the sequence of the large T-antigen of polyomaviruses, such as budgerigar fledgling disease virus and human polyomaviruses. Read-024 was detected using RT-PCR using the RNA extracted from virus-infected cells at 3 days p.i. (Fig. 2B), indicating that it was transcribed in infected cells. In addition, 16S ribosomal DNA of bacteria and mycoplasma was not detected in these DNA samples using PCR (data not shown). These results indicated that these read sequences obtained using RDV were parts of the viral genome.

Elongation of viral genomic sequences

Based on these viral nucleotide sequences, genome walking was performed using differential display RT-PCR (GeneFishing DEG Premix Kit; Seegene). We obtained DNA fragments of 5 and 2 kbp approximately. To obtain the entire genome sequence of this virus, we used the Genome Sequencer FLX System (Titanium) of Roche and 454 Life Sciences. Viral DNA was extracted by precipitation of 30-ml virus-infected cell supernatant at 4 days p.i using ultracentrifugation. The obtained 17,000 read sequences were analyzed using the GS *De novo* Assembler Version 2.3 (Roche) for *de novo* assembly. As a result, we obtained 15,131 total nucleotides with circular DNA forms comprising this viral genome (Fig. 3A). The viral genomic information was deposited in DDBJ/EMBL/GenBank (accession number AB543063). Organization of the viral genome is illustrated in Fig. 3B. Because we could not find a motif of replicative origin on this genome, the provisional nucleotide number is 1 in Fig. 3A and B. The locations of partial DNA fragments (read-024, -004A, and -004C) obtained using RDV and two long DNA fragments (5 and 2 kbp) obtained using genome walking are also illustrated in Fig. 3B. In addition, at least 15 predicted ORFs were found in both strands using GeneMark.hmm 2.0 (Fig. 3B). These ORFs, except for the large T-antigen-like ORFs, are not homologous to any genes of polyomavirus.

Regions homologous to polyomaviruses

The DNA sequence harbored an ORF encoding 698 amino acids; a region of this reading frame contains approximately 100 amino acids as determined using RDV. This ORF is homologous to the large T-antigen gene of avian polyomaviruses at ATP-binding region (E value of 8e-54) (Fig. 4A and B), although it is distinct from the usual configuration of polyomaviral T-antigen genes. Usually, T-antigen genes carry an intron in the middle of the sequence having one splice donor and two splicing acceptors, allowing alternative splicing to produce mRNA for large and small T-antigens. In contrast, the ORF appeared contiguous without introns, suggesting that the DNA is not a direct descendent of a polyomaviral DNA and likely belongs to a novel virus family. We provisionally named this DNA as JEE cells-infecting virus (JEECV).

Multiplicity of JEECV in JEE cells

To investigate multiplicity of JEECV in JEE cells, a TaqMan real-time PCR system was developed. Probe and primers were designed for the large T-antigen-like region. The virus stock at 0.01 $TCID_{50}$/cell multiplicity of infection (MOI) was inoculated into confluent JEE cells in a 24-well plate, and cells and supernatant were harvested at 24, 48, 72, 96, 120, 144, 163, and 187 h p.i. As illustrated in Fig. 5A, viral gene numbers increased in the cells and supernatant from 24 to 144 h p.i. Conventional PCR was also performed, and similar results were obtained (Fig. 5B).

Demonstration of intact genome size of JEECV

As illustrated in Fig. 3, 454 analysis revealed that JEECV genome is circular. We then performed rolling circle analysis for amplifying circular viral genomes (Johne, 2009). DNA extracted from the supernatant of virus-infected cells at 163 h p.i. (Fig. 4) was amplified using Phi29 enzymes (Templiphi) for circular DNA, and viral copy numbers were calculated for amplified products using real-time PCR (Fig. 4A). As a result, products of Templiphi were amplified approximately 128-fold compared with unamplified DNA (data not shown).

The reads using the next-generation sequencer were obtained as contiguous sequences (data not shown). To confirm that the circular viral genome exists, overlapping PCR on the viral genome was performed. DNA extracted from JEECV-infected cells was amplified using long PCR by overlapping the amplified region. As illustrated in Fig. 6A, we obtained PCR products at expected sizes. We confirmed the nucleotide sequences of bands after gel purification. This result suggests the presence of a circular viral genome in infected cells. In the viral genomic sequence, a repeat region is observed at 480–853 nt. The repeat region was sequenced within the long PCR product. Although we deposited a viral genomic sequence with three repeats in

Please cite this article as: Mizutani, T., et al., Novel DNA virus isolated from samples showing endothelial cell necrosis in the Japanese eel, *Anguilla japonica*, Virology (2011), doi:10.1016/j.virol.2010.12.057

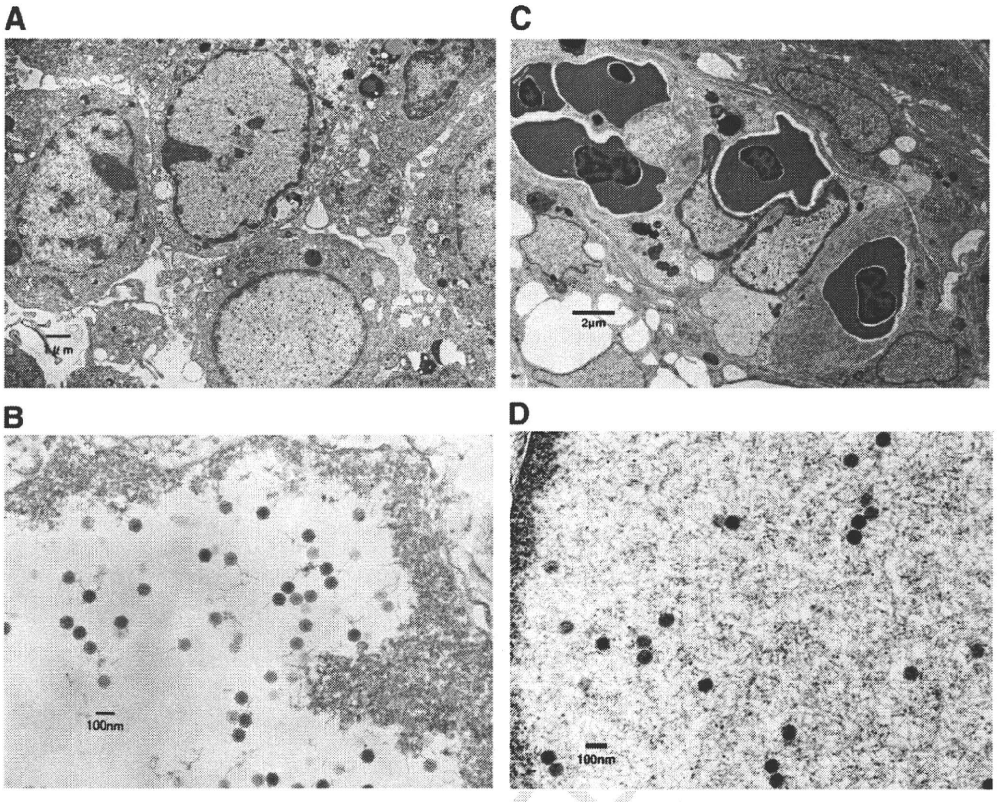

Q2 **Fig. 1.** Virus passage in JEE cells and infection in eels. 70th passage virus stock was infected to JEE cells (A and B) and healthy eel (C and D). EM photographs of B and D illustrate the enlarged images of A and C, respectively. Panels E and F illustrate gills and livers of virus-infected eel, respectively.

GenBank, we also detected two repeats using PCR (data not shown). Therefore, there should be different repeat numbers in virus-infected cells.

To further confirm the genomic DNA size of JEECV, we performed Southern blot analysis. DNA was digested using the restriction enzyme BglII, which is expected to induce a single cut in the viral genome at a position of 14418 nt. As indicated in Fig. 6B, a single band was found at approximately 15 kbp for BglII-digested DNA. Further confirmation is required with regard to the appropriate size for such large molecules of DNA. Another large-size DNA from nondigested DNA was observed after long exposure of the X-ray film. This band may represent another form of JEECV.

Detection of JEECV in eels

To confirm the infection of eels with JEECV, DNA was extracted from the gills of eels with natural VECNE and used to experimentally infect eels. PCR was performed for amplifying three different regions of viral genome. As illustrated in Fig. 7, viral genes were amplified in eels with natural VECNE and virus-infected eels, but not in healthy eels. Nucleotide sequences of these PCR products were confirmed after gel purification.

Discussion

In this study, we determined the genomic sequence of a novel eel virus, JEECV, which was isolated from eels with VECNE. The virus stock used in this study contained agent(s) that cause VECNE. Our results from 454 analysis, rolling circle amplification, and overlapping PCR suggested that JEECV genome is circular. We could not determine whether linear form exists in this study. Therefore, we believe that JEECV genome has two forms, linear and circular, in virus-infected cells. In addition, it is also possible that the entire linear form of the viral genome is longer than the present length obtained using Southern blot analysis. Viral genomic sequences in this study may represent one form of JEECV.

Interestingly, JEECV DNA contains regions homologous to the large T-antigen gene of polyomaviruses at ATP binding region, suggesting that this homologous region has biological function. We also investigated that bird polyomaviral T-antigen genes were more homologous to JEECV than mammals. Among four currently known bird polyomaviruses, avian polyomavirus, goose hemorrhagic polyomavirus (GHPV), finch polyomavirus, and crow polyomavirus (John and Muller, 2007), the diseases caused by GHPV (hemorrhagic nephritis and enteritis) resemble VECNE. JEECV large T antigen-like region also contains motifs conserved among polyomavirus T-antigens: DNAJ (HPDK) motifs, the canonical nuclear localization signal, and zinc finger motif. Conserved region 1 (CR1) motif was found in the C-terminus, instead of N-terminus where commonly found in the polyomaviral T-antigen (Pipas, 1992). It remains to be examined whether the T-antigen-like gene influences VECNE disease symptoms, as the T-antigen genes of polyomaviruses are known to be tumorigenic. We found that the transcript harboring the large T-antigen-like gene region was detectable, thus it is possible that the T-antigen gene product is expressed. Further investigation is needed to identify the structural and nonstructural viral protein ORFs in JEECV DNA and to determine the role of viral proteins, including the T-antigen-like gene, in the development of VECNE *in vivo*.

Recently, two novel viruses, bandicoot papillomatosis carcinomatosis virus (BPCV) 1 and 2, were detected from bandicoot (Bennett et al., 2008; Woolford et al., 2007, 2008 and 2009). These virus genomes have both T-antigens of an ancestral polyomavirus and the L1 and L2 capsid proteins of an ancestral papillomavirus. Inter-familial recombination was occurred between an ancient papillomavirus and an ancient polyomavirus more than 10 million years ago (Bennett et al., 2010). JEECV genome may also arise by recombination between a polyomavirus and a virus from unknown virus family.

Please cite this article as: Mizutani, T., et al., Novel DNA virus isolated from samples showing endothelial cell necrosis in the Japanese eel, *Anguilla japonica*, Virology (2011), doi:10.1016/j.virol.2010.12.057

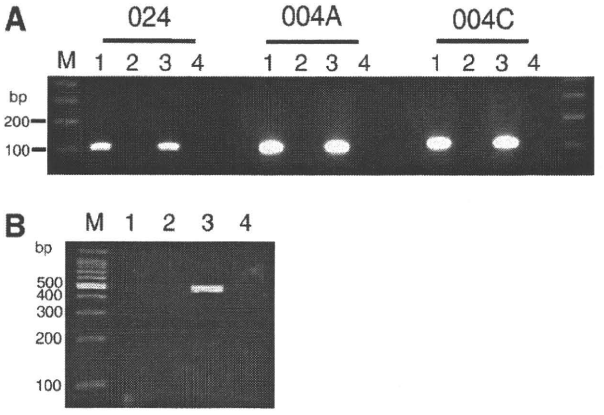

Fig. 2. Determination of viral genome sequence. A. Detection of viral DNA fragments. Three unknown DNA fragments (004A, 004C, and 024) are obtained using RDV. Primers are designed (004A-1 and -2, 004C-1 and -2, 024-3 and -4), and PCR is performed using the supernatant of virus-infected cultured cells at 7 days p.i. M, 100-bp DNA ladder marker; lane 1, supernatant of JEECV-infected cells; lane 2, supernatant of mock-infected cells; lane 3, JEECV-infected cells; lane 4, mock-infected cells. B. Detection of viral transcript. RT-PCR is performed using RNA extracted from virus-infected cells at 3 days p.i. to detect viral transcripts of the region harboring read-024 using PCR primers, 024-2 and 024-5. M, 100-bp DNA ladder marker; lanes 1 and 2, mock-infected cells; and lanes 3 and 4, JEECV-infected cells. Reaction of cDNA synthesis in lanes 2 and 4 is performed without Superscript III enzyme.

We are also keen to investigate in the possibility of latent infection by JEECV in Japanese eels. Natural VECNE is occasionally observed in kidneys or liver without symptoms in gills (data not shown). It is difficult to locate diseased eels exhibiting such weak symptoms. Therefore, we believe that there are eels latently infected by JEECV exhibiting very weak symptoms.

In a previous study, mortality after viral infection was reduced by incubating infected eels for more than 3 days at 35 °C under nonfeeding conditions (Tanaka et al, 2008). However, it is not cost-effective to treat a great number of eels with this condition simultaneously. To prevent the prevalence of VECNE, a monitoring system for JEECV infection developed in this study may be useful, if JEECV indeed causes VECNE.

Materials and methods

Cells, virus and viral infection

JEE cells were cultured in a medium containing Humedia-EB2 (Kurabo, Japan) and EGM-2 (Lonza, Switzerland) on a gelatin-coated 6-cm dish at 25 °C in a 5% CO_2 incubator. JEE cells were infected with the virus stock at 0.01 $TCID_{50}$/cell MOI. At 4 or 5 days p.i., the infectious fluid was harvested. To infect the eels with the virus experimentally, 1×10^6 $TCID_{50}$ (supernatant of virus-infected cultured cells) was inoculated intraperitoneally into healthy eels. At 10 days p.i., eels were analyzed. Tissues were homogenized using BioMasher (Wako Bio. Japan), and DNA was extracted using a QIAamp DNA mini kit. The experiments using eels were performed according to the regulations of Tokai University.

Analysis using RDV (Maeda et al., 2008; Mizutani et al., 2007)

The viral infected culture supernatant (100 μl) was centrifuged at 2000g, 15 min, 4 °C to remove cell debris and was treated with 0.0001 μg RNase A (Qiagen), and 10-μl Turbo DNA-free DNase I (Applied Biosystems, USA) were mixed with 1× Turbo DNA-free buffer and shaken at 37 °C for 30 min. For DNA extraction, a QIAamp DNA mini kit was used according to the manufacturer's instructions. A whole-genome amplification system (WGA; Sigma-Aldrich, USA) was used according to the manufacturer's instructions. In the RDV method, AmpliTaq Gold LD (Applied Biosystems) was used to obtain a high yield of the PCR products. We mixed 4 μl 10× amplification buffer in a GenomePlex Whole Genome amplification kit (WGA1) (containing primers, but no information on sequences) containing 5-μl DNA solution, 0.25 μl AmpliTaq Gold LD, and 30.75 μl distilled water. The reaction mixture was heated at 95 °C for 9 min (for activation of AmpliTaq Gold), followed by 70 cycles of amplification consisting of an annealing step at 68 °C for 1 min, a primer extension step at 72 °C for 5 min, and a denaturation step at 94 °C for 1 min. After the first DNA library was purified using the MonoFas DNA isolation system (GL Science, Japan), DNA was digested with 40-U *Hae*III (Takara Bio Inc.) at 37 °C for 30 min, and then the digested DNA was purified using MonoFas. To construct the second cDNA library, 2.50 μl DNA solution, 0.5 μl blunt *EcoR*I–*Not*I–*Bam*HI adapter (Takara Bio Inc.), and 3 μl ligation mix (Takara Bio Inc.) were reacted at room temperature for 30 min, and then the digested DNA was isolated using MonoFas. The second cDNA library was amplified using PCR using specially designed primer sets in which six nucleotides comprised CC (*Hae*III-digested sequence), and four variable nucleotides were added to the 3′ end of the adapter sequence. PCR was performed by mixing 15 μl AmpliTaq Gold PCR Master Mix containing AmpliTaq Gold, 0.5 μl forward primer, 0.5 μl reverse primer, 0.5 μl DNA solution, and 13.5 μl distilled water. The reaction mixture was heated at 95 °C for 12 min, followed by 70 cycles of amplification consisting of annealing and primer extension at 72 °C for 30 s and denaturation at 94 °C for 30 s. After electrophoresis of PCR products, DNA was isolated from the gel using MonoFas. Direct sequencing was performed using the forward primer and/or reverse primer.

Conventional PCR

For PCR, DNA and RNA were extracted from the supernatant and cells using the QIAamp DNA mini kit (Qiagen, USA). In this study, we used GoTaq Master Mix (Promega, USA) for conventional PCR. The reaction mixture contained 1× GoTaq Master Mix, 1 μl each of 50 μM forward and reverse primers, and template DNA. Primers are as follows:

004A-1 (5′-GGTCTCATGAAATGTAGATGTGCAGGTTAA-3′) and
004A-2 (5′-AATGCATATGAACGAGATATATACGAGC-3′) for 100-bp PCR products;
004C-1 (5′-CTCTCCGCCCTCCTGCTCATCCGGCTC-3′) and
004C-2 (5′-AATCAGACGCGCCTGAGCAGACCCAGCT-3′) for 110-bp PCR products;
024-1 (5′-TGTGATTTAGCGCAACGGCCGCAGCATA-3′) and
024-2 (5′-AGGCATCGCACATTAAACTGCACGCGCA-3′) for 240-bp PCR products; and
024-3 (5′-TACTGGTGTCTATTTGTTGCCGCACCTGC-3′) and
024-4 (5′-CAACGAACCCCGTAATTGGAATAAAGCGT-3′) for 121-bp PCR products. Usually, each PCR cycle involved denaturing at 94 °C for 2 min, annealing at 55 °C for 30 s, and primer extension at 72 °C for 30 s. This reaction was performed for 30–40 cycles. The nucleic acid sequences of PCR products were confirmed by direct sequencing.

For overlapping PCR, we used the iProof HF long PCR system (BioRad, USA). The reaction mixture contained 1× master mix, 0.2 μl each of 50-μM forward and reverse primers, and template DNA. Primers are as follows:

162F (5′-TCTGAATGCAATGTATGACTGAGATCC-3′) and
2821R (5′-ATCTGAGCTGCTGCGCCCAGGAAAGCTGG-3′) for 2659-bp PCR products;
2682F (5′-GACGCTTATGACGCTCCACTGGATGCGCAT-3′) and
6011R (5′-CTCTGCCATCTGAAGCCTCTTGCGCGTACC-3′) for 2940-bp PCR products;
5622F (5′-GGGACGTACCAGCGGAAGTACACACAATGA-3′) and

Please cite this article as: Mizutani, T., et al., Novel DNA virus isolated from samples showing endothelial cell necrosis in the Japanese eel, *Anguilla japonica*, Virology (2011), doi:10.1016/j.virol.2010.12.057